THE OHIO STATE UNIVERSITY

RESEARCH FOUNDATION

1314 KINNEAR ROAD COLUMBUS 12, OHIO

Report 467-Final

PROTECTION OF NIOBIUM AGAINST OXIDATION AT ELEVATED TEMPERATURES

G. M. Gordon and Rudolph Speiser
Department of Metallurgical Engineering

14 October 1961

Department of the Navy
Contract N6onr-222(28)

RF Project 467
Report - Final

FINAL

R E P O R T

by

THE OHIO STATE UNIVERSITY
RESEARCH FOUNDATION

Columbus 12, Ohio

To: DEPARTMENT OF THE NAVY
Office of Naval Research
Washington 25, D.C.
Contract N6onr-225(28)
Project (NR 039 005)

On: PROTECTION OF NIOBIUM AGAINST OXIDATION AT ELEVATED TEMPERATURES

Submitted by: G. M. Gordon and Rudolph Speiser
Department of Metallurgical Engineering

Date: 14 October 1961

NOTICES

When Government drawings, specifications, or other data are used for any purpose other than in connection with a definitely related Government procurement operation, the United States Government thereby incurs no responsibility nor any obligation whatsoever, and the fact that the Government may have formulated, furnished, or in any way supplied the said drawings, specifications, or other data, is not to be regarded by implication or otherwise as in any manner licensing the holder or any other person or corporation, or conveying any rights or permission to manufacture, use, or sell any patented invention that may in any way be related thereto.

The Government has the right to reproduce, use, and distribute this report for governmental purposes in accordance with the contract under which the report was produced. To protect the proprietary interests of the contractor and to avoid jeopardy of its obligations to the Government, the report may not be released for non-governmental use such as might constitute general publication without the express prior consent of The Ohio State University Research Foundation.

Qualified requesters may obtain copies of this report from the ASTIA Document Service Center, Arlington Hall Station, Arlington 12, Virginia. Department of Defense contractors must be established for ASTIA services, or have their "need-to-know" certified by the cognizant military agency of their project or contract.

ABSTRACT

A mechanism is proposed for the oxidation of a series of columbium-zirconium and columbium-zirconium-titanium alloys in air at temperatures above 700°C. This mechanism is based on the mode of nucleation of alpha zirconium from oxygen-saturated beta solid solution. Metallographic and x-ray diffractometric techniques were used in the formulation of the proposed mechanism.

TABLE OF CONTENTS

List of Figures

List of Figures (Cont'd)

List of Figures (Cont'd)

A STUDY OF THE OXIDATION MECHANISM IN Cb-Zr AND Cb-Zr-Ti ALLOYS AT ELEVATED TEMPERATURES

I. INTRODUCTION

Interest in columbium as a high temperature material has increased considerably in recent years. The metal possesses a rather unique combination of properties among which are too high-temperature mechanical characteristics; a very high strength-to-weight ratio at elevated temperatures; excellent fabricability; low thermal neutron absorption cross section; and relatively good corrosion resistance. The aforementioned properties make columbium potentially suitable for several design applications which have been severely limited to date from both an efficiency and performance standpoint. The major limitation has been the lack of available materials having the requisite characteristics. The main drawback to the current use of columbium as a high-temperature material is its poor oxidation resistance.

Zirconium, while it does not possess the superior high-temperature strength properties of columbium, does possess one of the lowest thermal neutron absorption cross sections of any of the readily available, relatively high melting point, corrosion-resistant metals. Thus, columbium-zirconium alloys should show excellent potential as nuclear reactor structural materials where low neutron cross section, good high-temperature strength, and good corrosion resistance are essential. Because of this potential, considerable research has been

devoted in the past several years to the study of the corrosion and oxidation characteristics of zirconium, and to the development of corrosion and oxidation resistant alloys.

The purpose of the present investigation was to gain some insight into the complex behavior undergone by one group of refractory metal alloys when heated in air. Such studies as the present should lead ultimately to the design of oxidation-resistant, high-temperature alloys on a more fundamental, less empirical basis.

II. EXPERIMENTAL PROCEDURE

A. MATERIALS

Various sources were employed for the metals used. Typical analyses for each metal are listed in Table I.

Table I. Typical Analysis of Metals Employed

Element	Per Cent Impurity			
	Fansteel High-Purity Cb Rod	Wah Chang Sintered Cb Rod	Mallory-Sharon Zr Bar	Chase Brass Iodide Ti
C	0.03	0.0050	----	0.016
Fe	0.005	0.0100	0.065	0.018
Si	0.01	< 0.0100	----	----
Ti	0.079	< 0.0150	----	----
Ta	0.16	0.1000	----	----
Ni	Trace	----	----	----
N	----	0.020	0.0052	----
B	----	< 0.0001	----	----
Cd	----	0.001	----	----
Cu	----	< 0.0040	----	----
W	----	< 0.0300	----	----
Zr	----	< 0.0500	0.03	----
Al,Mg,Mn,Mo, Pb,Sn,V,Zn	----	< 0.0020	----	----
O	----	----	0.072	0.026
H	----	----	0.0008	0.019

B. PREPARATION OF SPECIMENS

The metals used were cold-rolled into sheets, cut into small pieces, and degreased in trichloroethylene. The constituents to be melted were placed in a tungsten electrode arc-furnace. The melting was performed under a gettered argon atmosphere. To insure homogenization, the samples were remelted five times before removal from the furnace. The arc-melted buttons were limited in weight to about six grams. For oxidation testing, rectangular prism specimens about 3/8-inch x 3/8-inch x 1/8-inch were prepared from these buttons by grinding and wet-polishing through 600-grit silicon carbide paper.

On those specimens where an x-ray investigation was contemplated, greater surface area was required than could be obtained directly from an arc-melted button. To produce these larger specimens, the arc-melted buttons were remelted under argon in a levitation melting furnace, Fig. 1, and were cast into plates. Flat specimens about 0.6-inch x 0.6-inch x 0.1-inch were then machined from these plates and prepared in the same manner as the arc-melted specimens.

In all cases, the weight losses occurring in either melting process were less than 0.1%. Thus, the alloy compositions reported in this investigation are believed accurate.

C. OXIDATION

Oxidation testing was performed in a modification of the apparatus designed by McCullough, Beck, and Fontana.[1] The equipment consists of a vertical tube "globar" furnace, a magnetically damped analytical balance mounted above the furnace on an independent, vibration damped

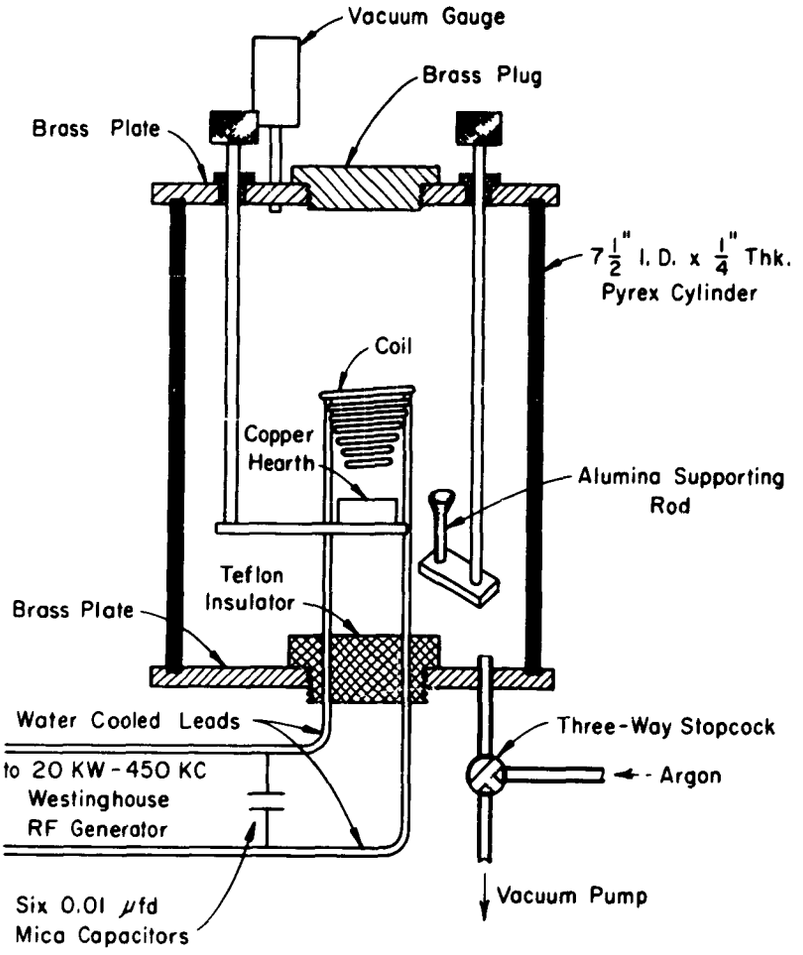

Fig. 1. Sectional view of the levitation-melting furnace

angle iron frame, Fig. 2, an air-drying train, and a temperature recorder-controller set-up. The analytical balance was placed on a small movable platform and could be rolled back to allow the suspension wire to be lowered in and out of the furnace without bending. The temperature could be controlled within ±2°C.

Periodic weight readings were taken and recorded during the runs. Dry air was used and the air-flow rate was set at 50 cc per second (S.T.P.). During the weighings the air flow was diverted from the furnace by means of a two-way stop-cock.

D. METALLOGRAPHIC PREPARATION

Specimens were held in two types of mounts for polishing. When a plane surface was desired, the specimen was placed in a brass clamp and held in place with set screws. This method was not too useful, however, when it was necessary to retain the outermost oxides intact. To do this, the specimen was placed in a mold and mounted in a room temperature setting epoxy resin. The mold was placed in a vacuum dessicator and the atmosphere was evacuated with a mechanical pump. Entrapped gases were bubbled out, allowing the epoxy resin to flow into the sometimes porous outer oxides.

The specimens were polished through 600-grit silicon carbide on a wheel using paper disks under flowing water. This was followed by polishing consecutively on paraffin and "microcloth" using 5- and 0.1- micron alumina, respectively.

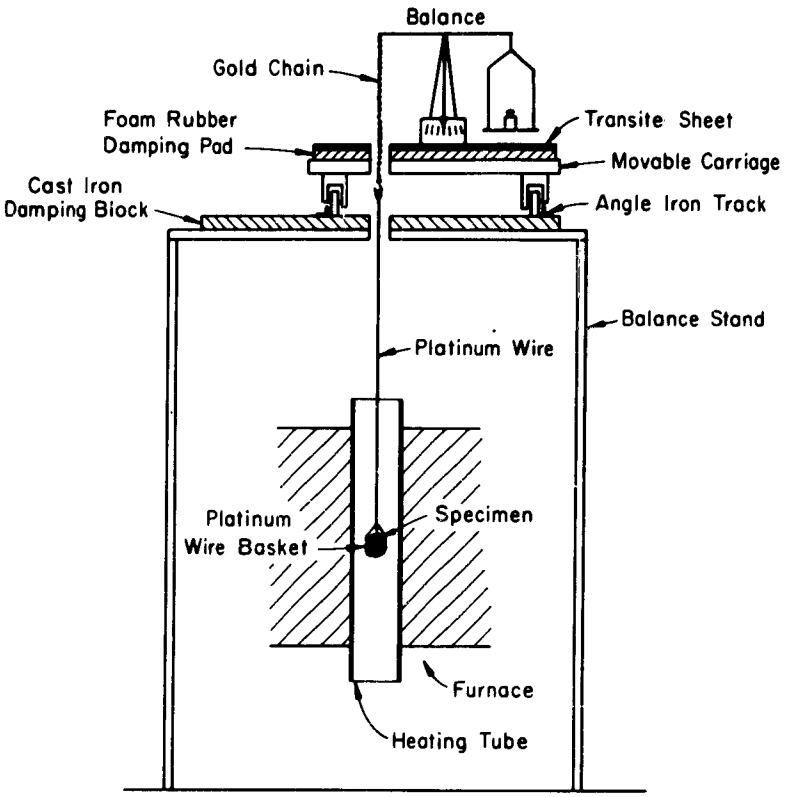

Fig. 2. Schematic diagram of the oxidation furnace with method of sample suspension

On those specimens where etching was desired, the etchant used consisted of 50 parts by volume nitric acid to 50 parts water and 1 part hydrofluoric acid.

E. X-RAY DIFFRACTION

An x-ray diffractometer using nickel filtered copper $K\alpha'$ radiation, was used to identify the oxide phases present in situ. The oxidized specimens were first sectioned and polished normal to the large plane surfaces and photomicrographs of the oxide layers were taken. An x-ray traverse of the surface was made, the peak intensity versus the Bragg 2θ angle being recorded on a strip-chart recorder. After completing a traverse, the surface of the sample was ground to a sufficient depth to expose the next visible reaction layer.

X-ray traverses at successively increasing depths were made until only the unoxidized specimen center remained. It was not always possible to grind parallel to the original outer surface, therefore, some overlapping of zones occurred. X-ray data obtained by this method are subject to any preferred orientation effects which may exist in the specimen. Hence, the relative line intensities may vary considerably from those obtained on a randomly oriented sample.

In an attempt to concentrate the internally dispersed oxide phases and to obtain them in a randomly oriented manner, a second method involving chlorination was used. One side of the specimen was ground to the unreacted core to allow the chlorine direct access to the metallic phases. The sample was set in an alumina boat which was placed in the glass reaction tube of the set-up shown in Fig. 3. This apparatus

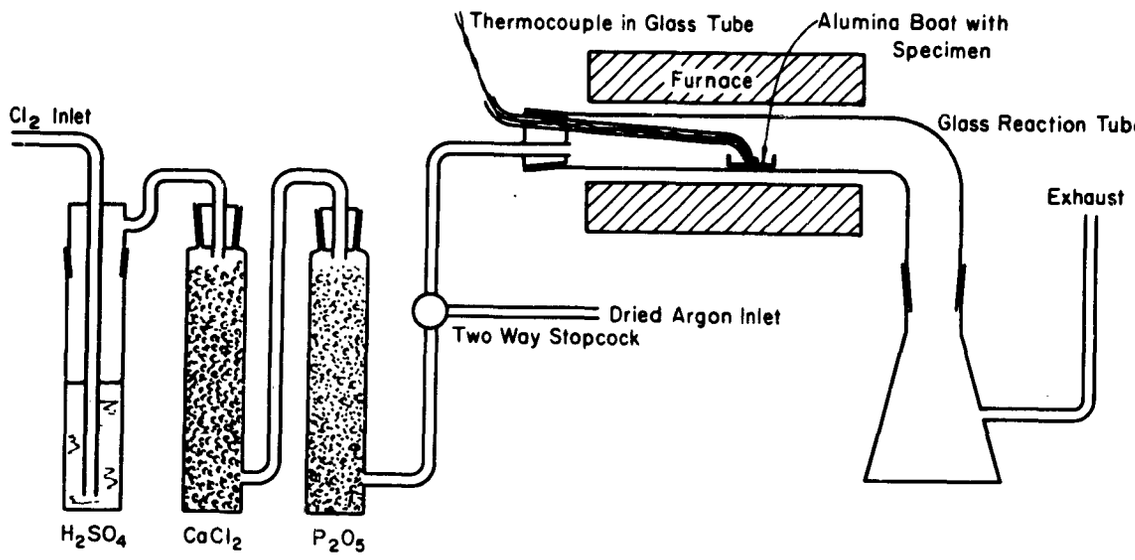

Fig. 3. Schematic diagram of the chlorination apparatus

is similar to one described by Colbeck, Craven, and Murray[2] for the isolation of inclusions in iron alloys.

The oxide powder obtained after chlorination was placed in a thin-walled glass capillary tube and a powder pattern was taken using copper Kα radiation.

III. EXPERIMENTAL RESULTS

A. OXIDE MORPHOLOGY

Upon metallographic examination, it was found that columbium-zirconium and columbium-zirconium-titanium alloys undergo a dual type of oxidation, yielding not only the normally expected external oxides, but also a zone of internal oxidation. For the purposes of this investigation, internal oxidation is defined as oxidation occurring within an alloy due to oxygen penetration and resulting in the isothermal formation of multiphase regions in which one or more phases are metallic, the remainder being oxides.

The morphology of the internally oxidized regions in the alloys studied was highly varied. Figure 4 is a 200 magnification photo taken of a 50 a/o Zr, 45 a/o Cb, 5 a/o Ti alloy which had been oxidized for 50 hours at 1000°C. The indentations are from a microhardness traverse and show the extreme variation in hardness across the various zones. Before oxidation the alloy contained only β solid solution, the equilibrium structure for columbium-zirconium binary alloys at 1000°C.[3] The addition of 5 a/o Ti does not appear to cause second-phase formation. Titanium is completely soluble in both columbium and zirconium.[3]

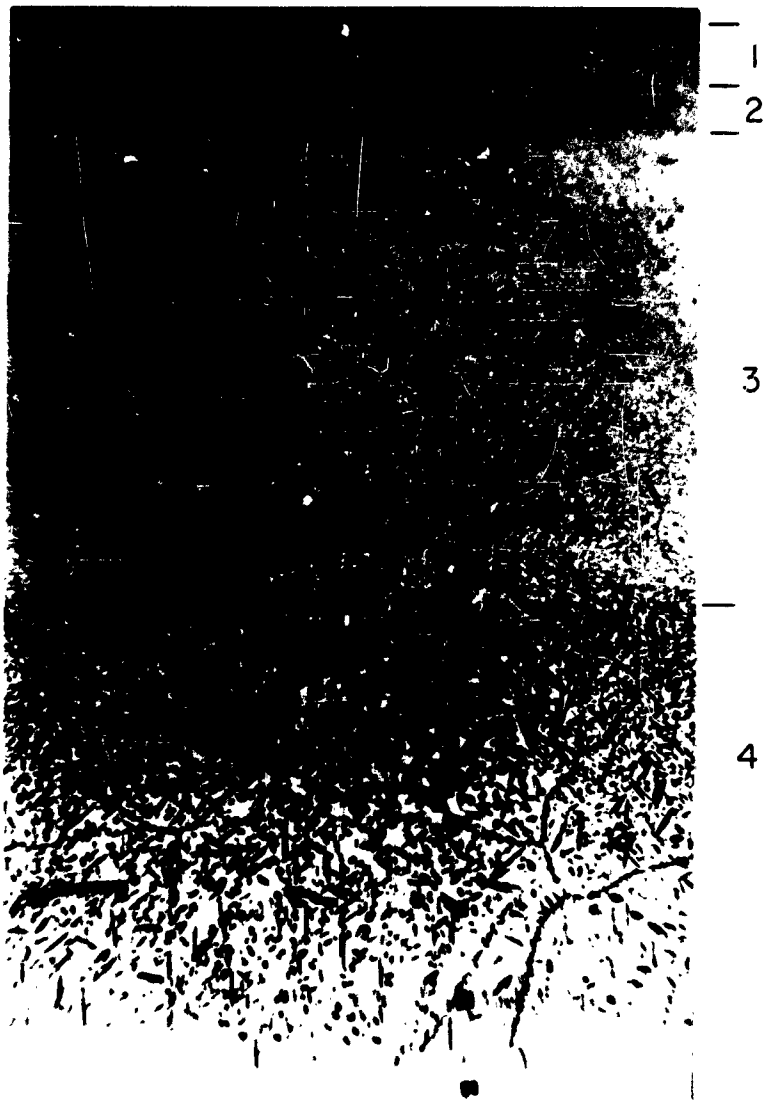

Fig. 4. Section through a 50 a/o Zr, 45 a/o Cb, 5 a/o Ti alloy oxidized in air for 50 hours at 1000°C (200X)

On the oxidized alloy Fig. 5, there are four distinctly different zones visible. The identification of the various phases present in these regions was performed using x-ray diffraction techniques. The two outer layers, zones 1 and 2, consist only of oxide phases. These two zones actually contain four two-phase layers, although the interfaces between layers are not always distinguishable. The outermost layer consists of Cb_2O_5 plus the double oxide $6ZrO_2 \cdot Cb_2O_5$. The second layer contains CbO_2 plus $6ZrO_2 \cdot Cb_2O_5$. Next is a layer of CbO_2 plus monoclinic ZrO_2 and finally a region containing CbO plus ZrO_2.

Zones 3 and 4 are shown more clearly at 2000 magnification in a continuous traverse across the oxidized section, Fig. 5. It may be seen that zone 3, the internally oxidized zone, is an oxide dispersion in a solid solution matrix. The morphology of the dispersion varies continuously towards the specimen center, appearing as a very fine pearlitic structure at the zones 2 and 3 interface, the lamellar structure gradually coarsening and changing to a more massive blocky precipitate at the zones 3 and 4 interface. The dark phase is monoclinic ZrO_2 and the lighter phase is columbium-rich β solid solution. A pearlitic structure is also visible in zone 2.

The core, zone 4, contains a two-phase metallic structure in the region of the zones 3 and 4 interface. The oriented second phase, α-zirconium, precipitates within the grains and at the grain boundaries near the internal zone interface. Toward the center of the specimen the intragranular α phase gradually thins out, leaving the grain boundaries outlined by precipitate which finally disappears. The sharpness

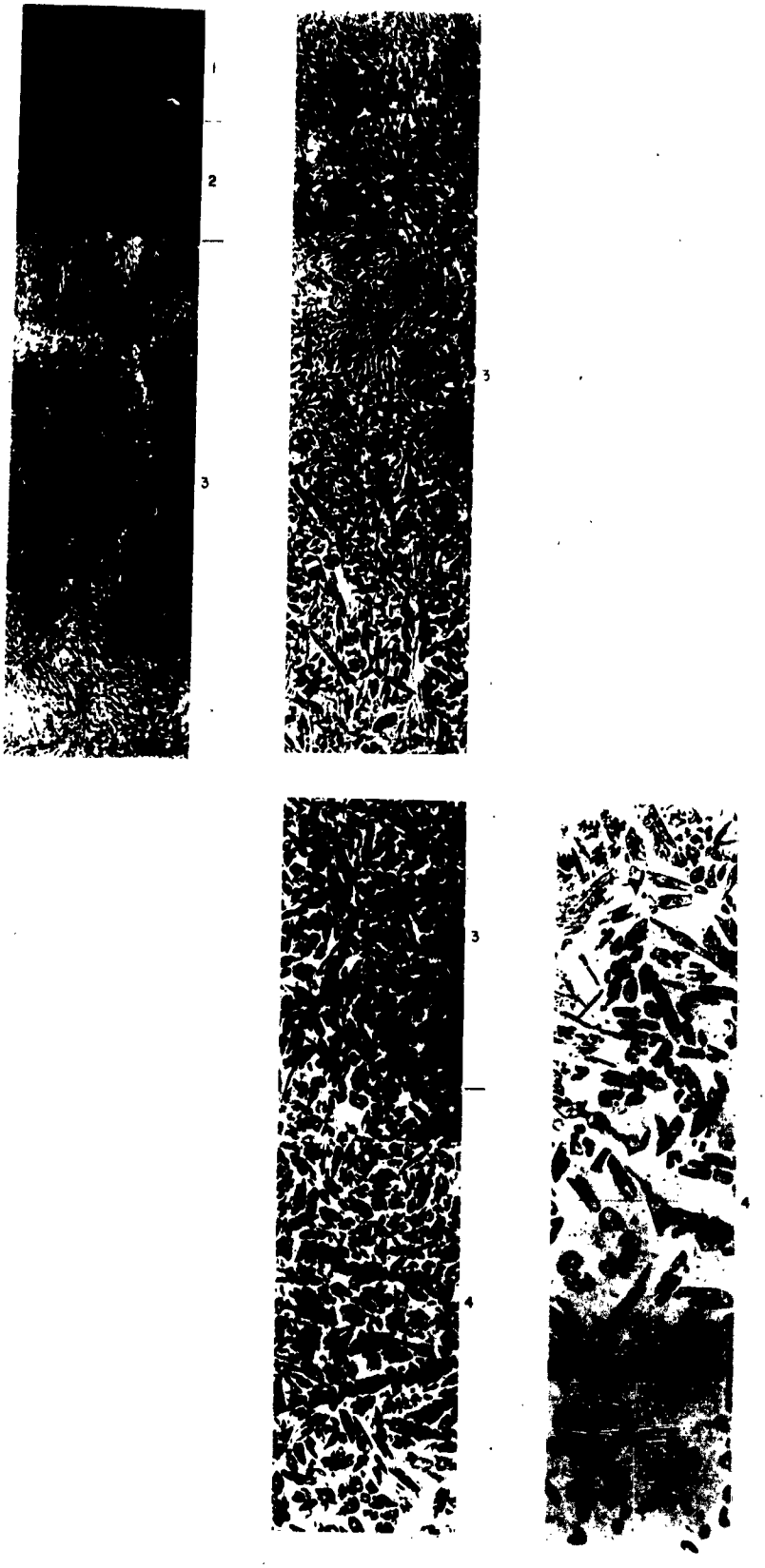

Fig. 5. Section through a 50 a/o Zr, 45 a/o Cb, 5 a/o Ti alloy oxidized in air for 50 hours at 1000°C (2000X)

of the zones 3 and 4 interface indicates that the intragranular oxygen penetration is highly isotropic with respect to grain orientation.

There appear to be no "aging" effects within the internally oxidized zone, that is, there is no noticeable tendency for the initially formed, very fine structure to agglomerate and coarsen with time.

The oxide morphology of a typical binary alloy may be seen in Figs. 6 and 7. These photos were taken of a 57 a/o zirconium, 43 a/o columbium alloy which had been oxidized 16.6 hours at 1000°C. It may be seen from Fig. 6 that the binary alloys also undergo internal oxidation. The alloy has one additional region near the core. This region, as well as zone 4, contains alpha plus beta, but the alpha-phase precipitate in this case probably came out on cooling and possesses a somewhat different morphology. Fig. 7 at 2000 magnification is a continuous traverse across the internal region, zones 2, 3, and 4. The pearlitic structure is seen to exist in the binary Cb-Zr alloys as well as in the Ti-containing ternary alloys investigated. The same phase regions appear in both the binary and ternary alloys, indicating that titanium additions remain in solution, their principal effect being in regulating the thickness of the outer oxides.

The effect of titanium on outer oxide thickness is shown in Fig. 8 which contains photos of four 40 a/o zirconium alloys in which the titanium contents are 0, 1, 5, and 10 a/o, respectively, the balance being columbium. All four alloys were oxidized about one hour at 1000°C. On the zero and one atomic percent titanium alloys there is

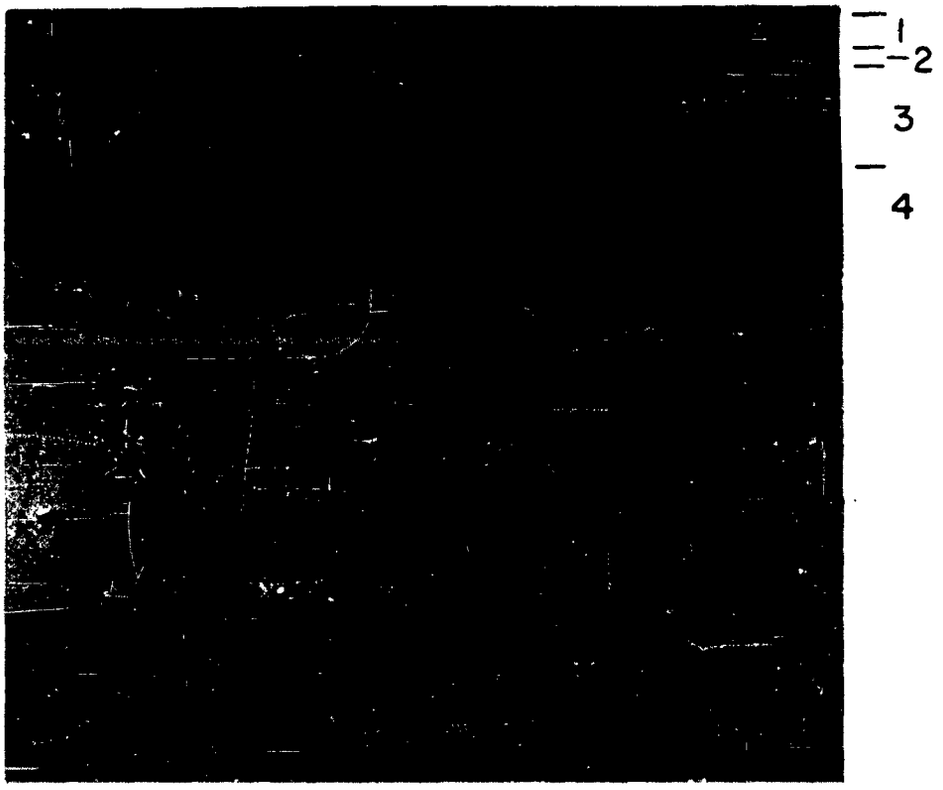

Fig. 6. Section through a 57 a/o Zr, 43 a/o Cb alloy oxidized in air for 16.6 hours at 1000°C (100X)

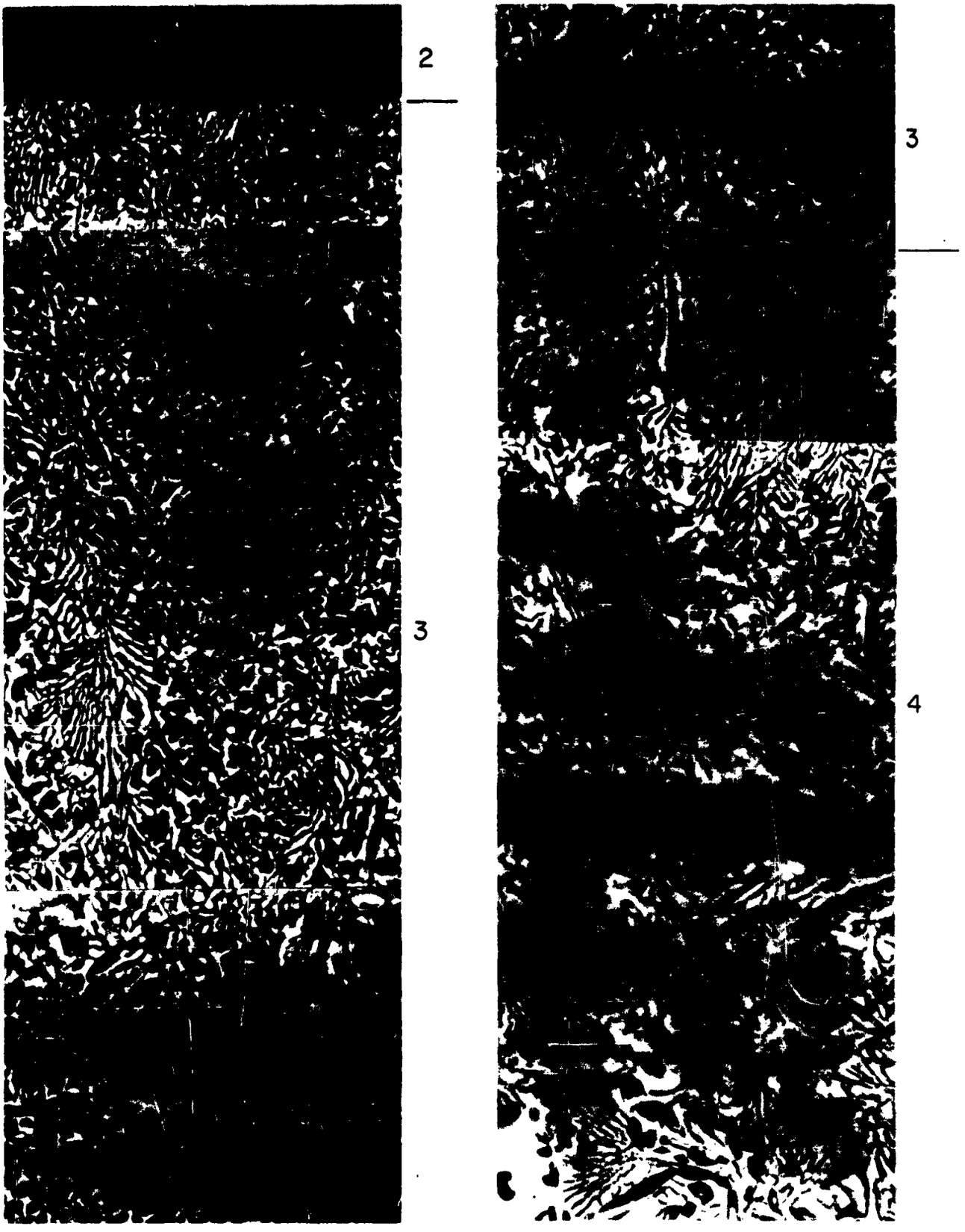

Fig. 7. Section through a 57 a/o Zr, 43 a/o Cb alloy oxidized in air for 16.6 hours at 1000°C (2000X)

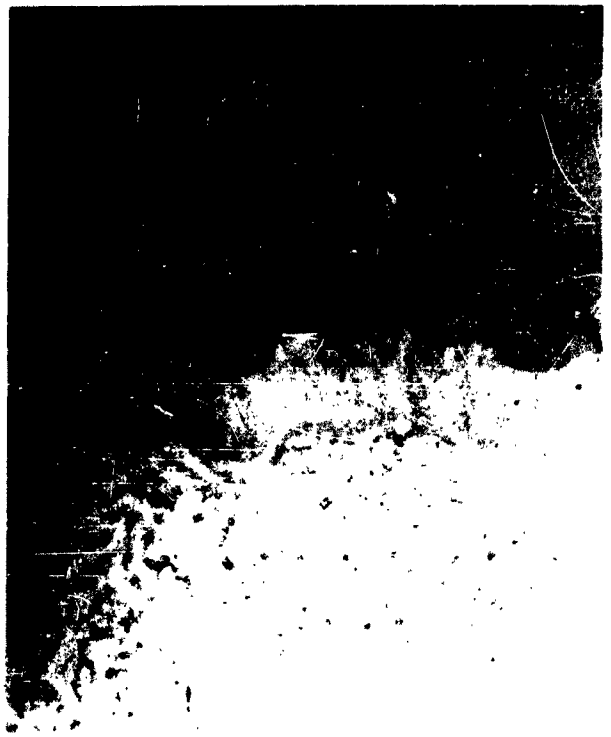

40% Zr - 60% Cb (1.4 hours)

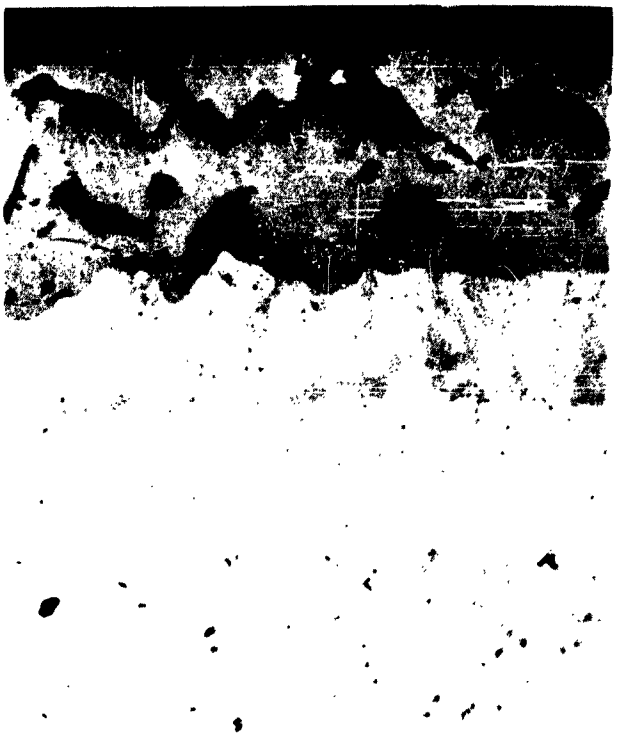

40% Zr - 59% Cb - 1% Ti (1.2 hours)

40% Zr - 55% Cb - 5% Ti (1.6 hours)

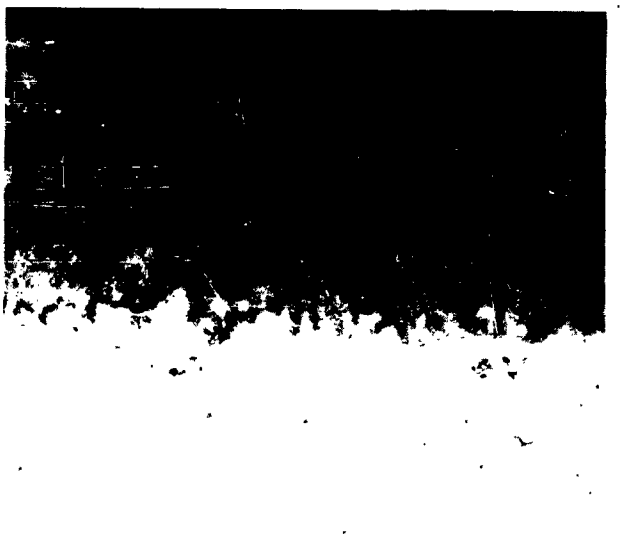

40% Zr - 50% Cb - 10% Ti (1.0 hours)

Fig. 8. Sections through four 40 a/o Zr alloys oxidized in air for about one hour at 1000°C (200X)

a very thick, porous, outer oxide consisting of Cb_2O_5 plus $6ZrO_2 \cdot Cb_2O_5$ and a thinner internal zone consisting of a lamellar dispersion of ZrO_2 in a β solid solution matrix.

The outer oxide on the 5 a/o Ti alloy is considerably thinner and on the 10 a/o Ti specimen it has virtually disappeared. A comparison of Fig. 9, a 55 a/o Cb, 45 a/o Zr alloy oxidized about two hours at 1000°C with the 55 a/o Cb, 40 a/o Zr, 5 a/o Ti alloy of Fig. 8 shows that, for two alloys of the same columbium content, titanium is considerably more effective in cutting down the rate of outer oxide growth than is zirconium.

On the alloys studied, growth of the outer oxides appears dependent on the prior formation of an internally oxidized zone. This may be seen in Figs. 5 and 7. In zone 2, a region consisting of CbO plus ZrO_2 near the zones 2 and 3 interface, a lamellar skeleton remains, indicating that zone 2 is growing into the internal zone. In those alloys where the thick porous oxide exists, zone 2 is apparently converted almost immediately into the outer higher oxides due to the direct access of oxygen to the CbO. The continuity between the ZrO_2 in the internal zone and the external scale is believed to be the main reason the external scale is so tenacious on thermal cycling.

In the higher zirconium alloys, the ratio of ZrO_2 to solid solution in the internal zone increases as might be expected. This is illustrated in Figs. 10 and 11. Figure 10 is a 200 magnification photo of a 70 a/o Zr, 20 a/o Cb, 10 a/o Ti alloy oxidized 2.3 hours at 1000°C.

Fig. 9. Section through a 55 a/o Cb, 45 a/o Zr alloy oxidized for about 2 hours at 1000°C (200X)

Fig. 10. Section through a 70 a/o Zr, 20 a/o Cb, 10 a/o Ti alloy oxidized in air for 2.3 hours at 1000°C (200X)

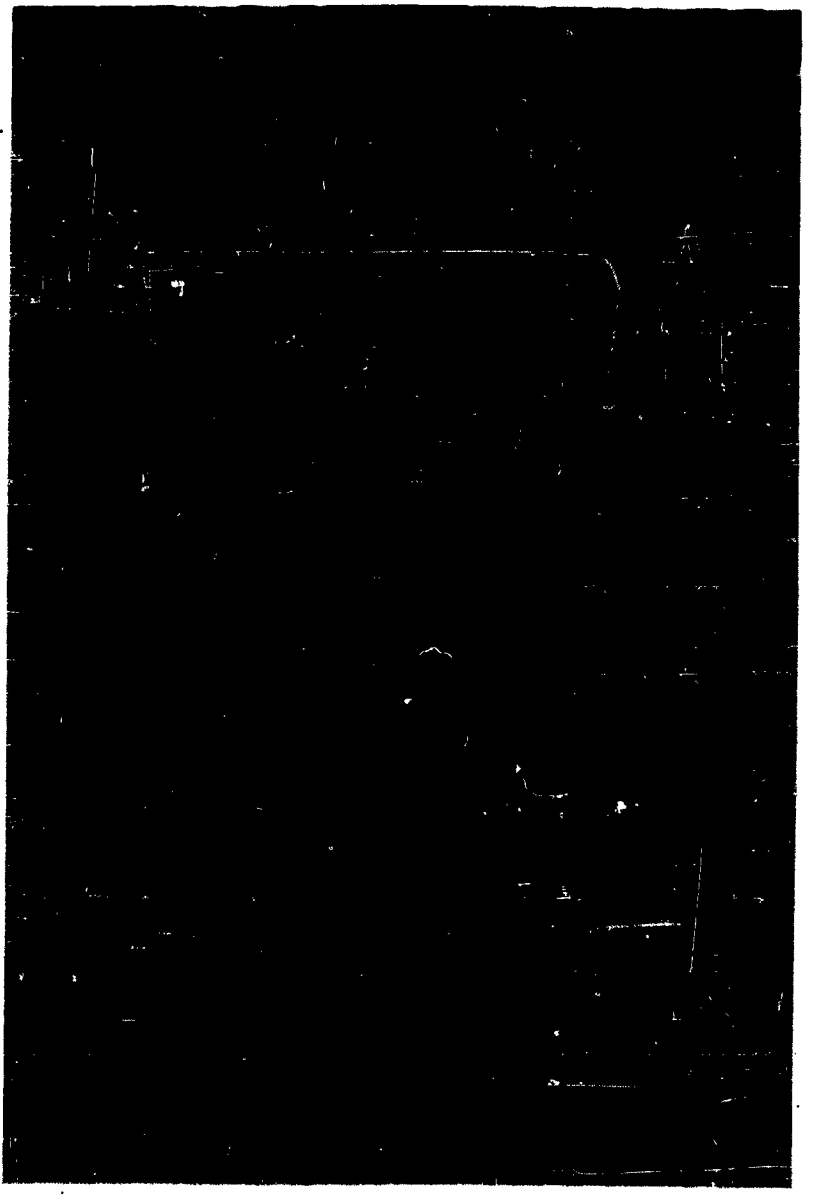

Fig. 11 Section through a 70 a/o Zr, 20 a/o Cb, 10 a/o Ti alloy oxidized in air for 2.3 hours at 1000°C (2000X)

The α phase precipitating in the core comes out in an oriented acicular form. The internally oxidized region, zone 3, contains almost all oxide. This is shown in Fig. 11, a 2000 magnification photo of zones 3 and 4. In zone 3 in the region of the zones 3 and 4 interface, the ZrO_2 is precipitating in the form of long rods, oriented normal to the interface and separated by very thin regions of β solid solution. The acicular α phase has started to break up and spherodize near the zones 3 and 4 interface. It appears that some of the α phase has gone back into solution indicating that an alpha concentration gradient may exist at the interface region of the core. The black spots in zone 3 of Fig. 10 are voids which were probably formed during oxidation, but which became enlarged during metallographic polishing.

In describing the morphology of the previous alloys, we have assumed that internal oxidation at temperature occurred, and not just oxygen penetration and subsequent precipitation upon cooling to some temperature at which the solubility limit was exceeded. This assumption is verified by the continuity of structure between the outer oxides and the internal zone as shown in Fig. 7. Since the outer oxides must have existed at temperature, it is obvious that the internal zone did likewise.

B. OXIDATION KINETICS

All alloys studied were found to follow a kinetic expression of the following type, at least during the first several hours of oxidation;

$W = kt^n$, where W is the weight gain per unit of original surface area, k is a rate constant, t is the time and n is an exponent which is characteristic of the oxidation mechanism and is generally equal to 0.5 for a "diffusion-controlled" oxidation process. If the weight gain versus time data are plotted on log-log graph paper, straight lines will result having slopes equal to n and the magnitude of W at t = 1 hour will give the rate constant, k.

A typical log-log plot for a 60 a/o Zr, 39 a/o Cb, 1 a/o Ti alloy appears in Fig. 12. The data points approximate a straight line of slope 0.37. Values of n and k for a series of columbium-zirconium-titanium alloys are given in Table II and Figs. 13 and 14. Figure 13 is a plot of n versus a/o zirconium for a series of constant titanium parameters. It may be seen that for the columbium-zirconium binary alloys there is a rapid decrease in exponent between 0 and 10 a/o Zr, the value decreasing from 0.79 to 0.53. For all titanium contents indicated, there is also a pronounced decrease in the exponent, n, between 45 and 50 a/o zirconium. Beyond the rapid drop off in exponent, an approximately constant n value is obtained up to at least 70 a/o zirconium. The minimum slope obtained was 0.23, and was for a 50 a/o Zr, 40 a/o Cb, 10 a/o Ti alloy.

For a constant zirconium content, the exponent is seen to decrease in going from 0 to 10 a/o Ti. One alloy containing 15 a/o titanium (50 a/o Zr, 35 a/o Cb, 15 a/o Ti) was tested and gave an exponent of 0.31, a value higher than the corresponding values of the 5 and 10 a/o titanium alloys, indicating that a minimum in slope for a given zirconium content is probably reached between 5 and 15 a/o titanium.

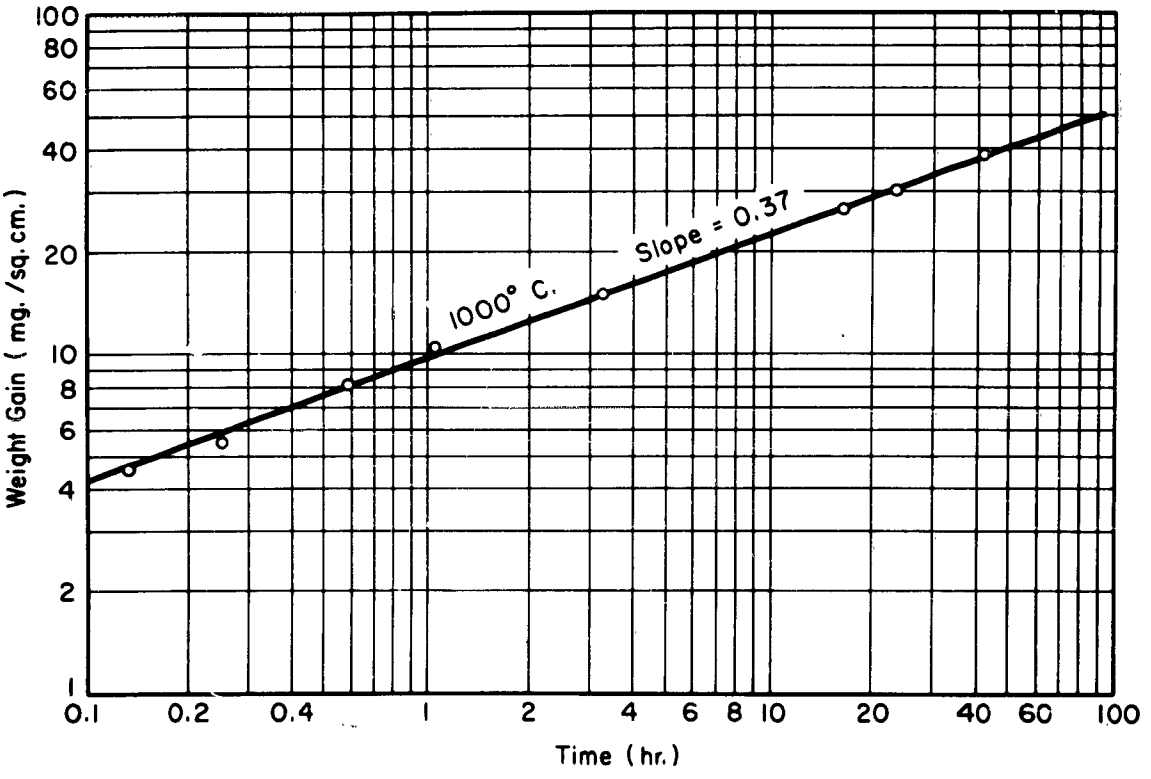

Fig. 12. Weight gain versus time plot for a 60 a/o Zr, 39 a/o Cb, 1 a/o Ti alloy

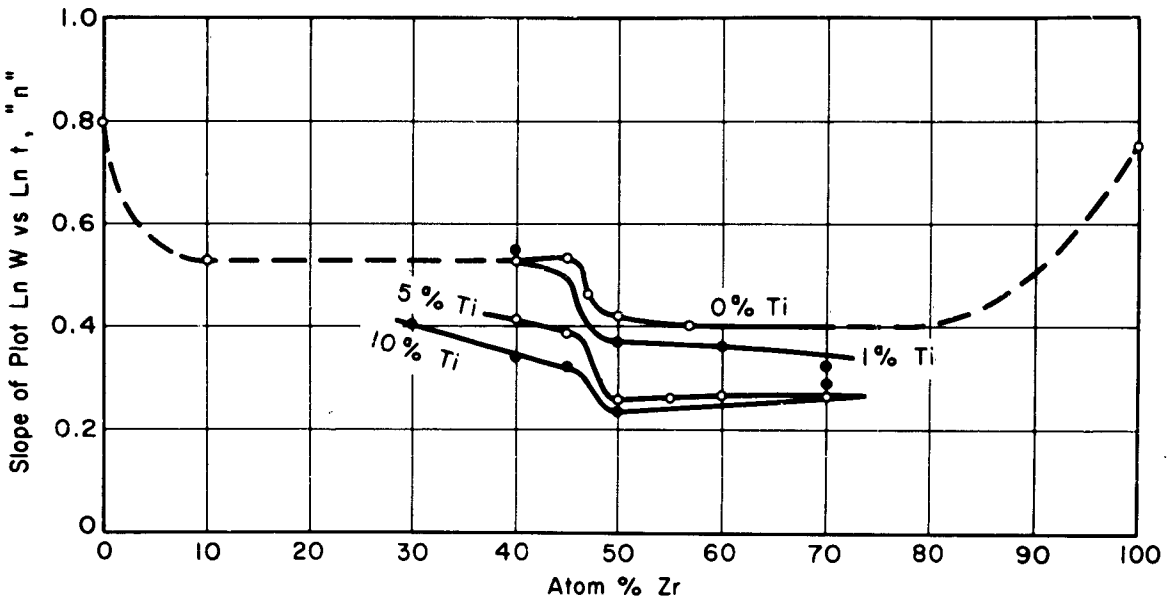

Fig. 13. Slope of ln W .s ln t plot, "n", versus atomic percent zirconium plot for a series of alloys oxidized at 1000°C

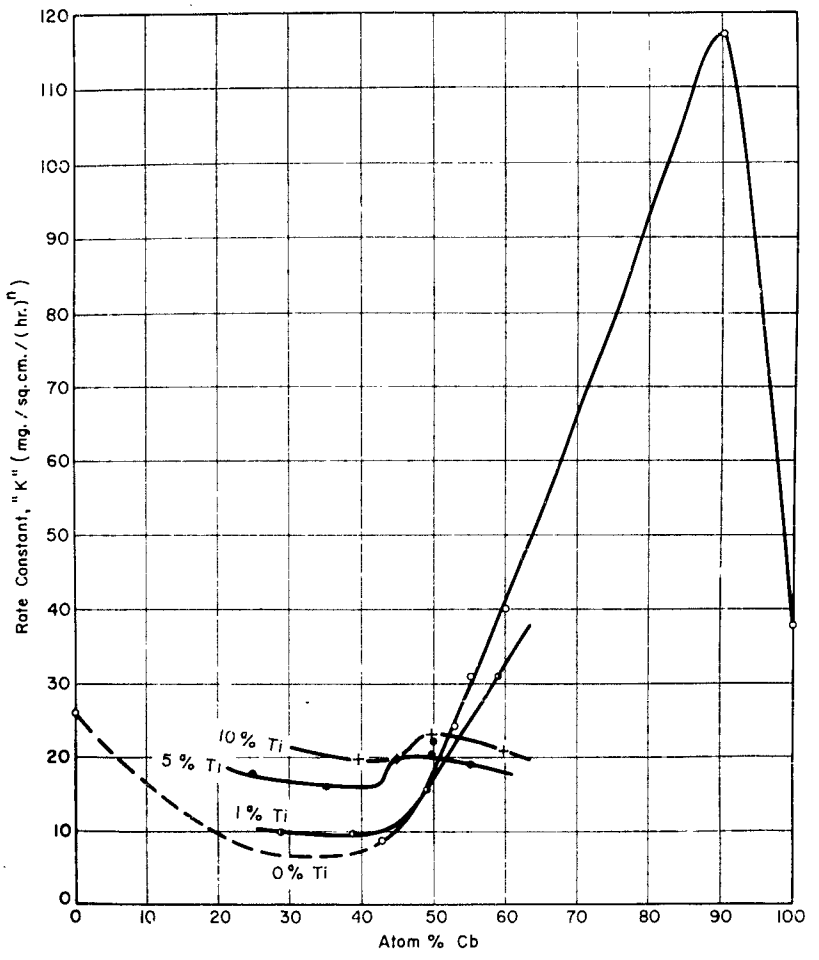

Fig. 14. Rate constant, "k", versus atomic percent columbium plot for a series of alloys oxidized at 1000°C

Table II. Slopes n and Intercepts k (at 1 hour) of the ln W vs. ln t Curves for a Series of Cb-Zr-Ti Alloys Oxidized in Air at 1000°C.

Alloy Composition (a/o)			Slope n	One-hour Intercept k, $mg/cm^2\text{-}hr^n$
Cb	Zr	Ti		
100	0	0	0.79	38.0
90	10	0	0.53	117.0
60	40	0	0.53	40.3
55	45	0	0.53	31.0
53	47	0	0.47	24.4
50	50	0	0.42	22.3
43	57	0	0.41	9.5
59	40	1	0.55	31.0
49	50	1	0.37	15.9
39	60	1	0.37	9.7
29	70	1	0.33	10.2
55	40	5	0.42	19.1
50	45	5	0.39	20.3
45	50	5	0.26	19.8
40	55	5	0.27	15.5
35	60	5	0.27	16.2
25	70	5	0.26	18.1
60	30	10	0.40	20.7
50	40	10	0.34	23.2
45	45	10	0.32	20.0
40	50	10	0.23	19.7
20	70	10	0.30	28.0
35	50	15	0.31	24.5
0	100	0	0.75	26.0

The rate constant k is seen to vary in a somewhat less orderly manner with composition, Fig. 14, than is the exponent. For binary alloys, k is found to go through a minimum at about 35 a/o columbium, and then to rise very rapidly to a maximum value of at least 117 mg/cm^2-hr at about 90 a/o Cb. The maximum value is in approximate agreement with the data presented by Klopp, Sims, and Jaffee.[4] They found a maximum 1000°C rate of 135 $mg/cm^2/hr$ at about 95 a/o columbium. However, their data were based on an average rate after five hours at temperature. This was done assuming linear oxidation, i.e., n = 1, whereas the authors find an exponent of 0.53. Thus, the two rate constants are not directly comparable.

The addition of titanium to columbium-zirconium alloys increases the value of k at lower columbium contents and decreases it at higher contents. For all titanium contents investigated the rate constant appears to increase rapidly between 40 and 50 a/o columbium, although for the 5 and 10 a/o titanium alloys, the magnitude of the increase is considerably reduced.

It is doubtful that any fundamental significance can be attached to the rate constant in nonparabolic and nonlinear cases, especially since the dimensions of the rate constant are a function of the exponent, n. However, from a practical standpoint, k represents the weight gain per unit area after one hour at temperature and is thus a basis for comparison of the short-time, weight-gain behavior of the various alloys.

The oxidation resistance, as measured by weight-gained, for the best alloys studied was considerably better than that for either pure columbium or pure zirconium. For example, for a 45 a/o Cb-50 a/o Zr-5 a/o Ti alloy, the weight-gained after 100 hours at 1000°C was about 5% that of pure columbium and 9% that of pure zirconium.

A log-log plot of zone thickness in mils versus time in hours for a 50 a/o Zr, 45 a/o Cb, 5 a/o Ti alloy oxidized at 1000°C appears in Fig. 15. This alloy was found to oxidize according to the general weight-gain expression, $W = kt^n$. Zone thicknesses were measured from photomicrographs taken of a series of specimens which had been oxidized for various times at the same temperature. The depth of penetration versus time relationship for the internal zone of this alloy was found to be very similar to the over-all weight-gain versus time expression, the exponents being 0.23 and 0.26, respectively. This was to be expected since by far the greatest portion of the weight-gain was due to ZrO_2 formation in the internal zone, a region which after 10 hours at temperature is about eight times thicker than all the outer oxides combined. The outer oxides were found to follow an approximately parabolic relationship, the exponent being 0.44. For this alloy the kinetic behavior at 1000°C may be represented by the following equations if we assume the weight-gain is proportional to the layer thickness.

$$W = k_1 t^{m1} + k_2 t^{m2} \qquad (1)$$

$$W = k_3 t^n \qquad (2)$$

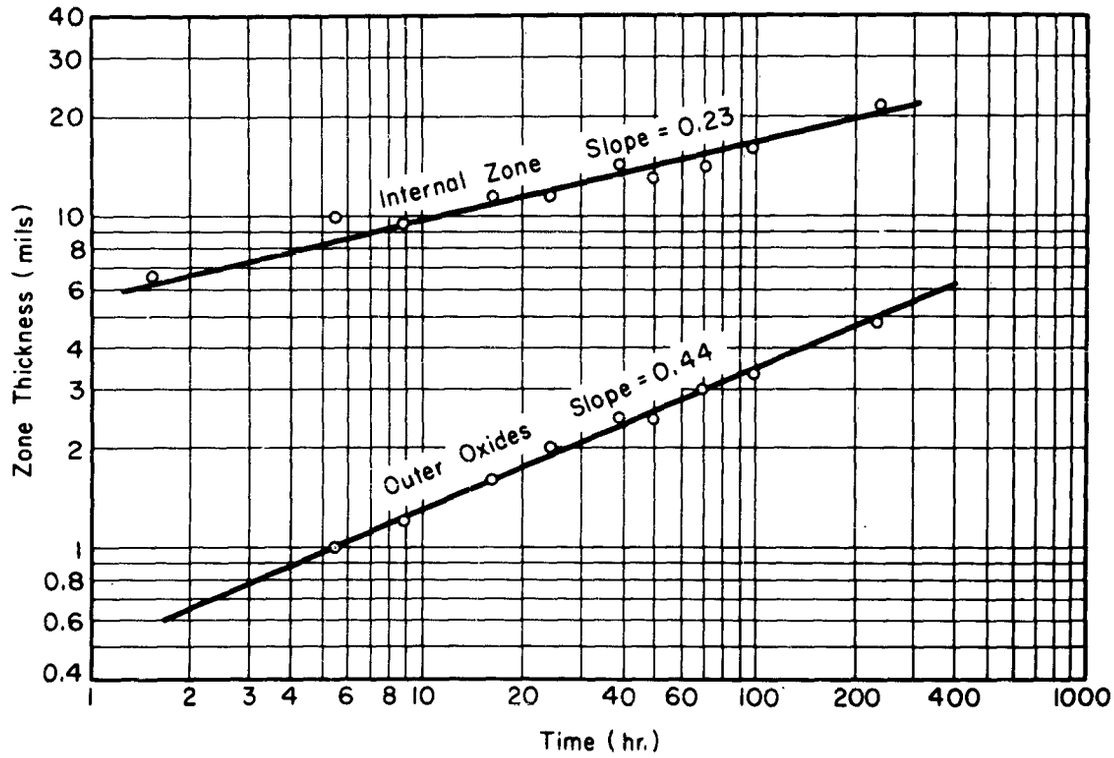

Fig. 15. Zone thickness versus time plot for 50 a/o Zr, 45 a/o Cb, 5 a/o Ti alloys oxidized in air at 1000°C

Solving for the constants from the experimental data, the above equations become,

$$W = \underbrace{0.9t^{0.44}}_{\text{external}} + \underbrace{19.1t^{0.23}}_{\text{internal}} \qquad (3)$$

$$W = \underbrace{19.8\ t^{0.26}}_{\text{overall}} \qquad (4)$$

A comparison of the weight-gain versus time plot determined experimentally and that calculated from zone thickness measurements using Eq. (3) is shown in Fig. 16. The agreement between the experimental and calculated curves is excellent for times extending to at least 240 hours.

Knowing the values of the two rate constants in Eq. (3), it is possible to obtain an estimate of the fraction of the total weight-gain due to the external oxide scale and to the internally oxidized zone. After one hour at temperature only about 5% of the total weight-gain is due to the external scale. This percentage increases and after 240 hours about 15% of the total weight-gain is external. These estimates include the ZrO_2 in the external scale which was formed by internal oxidation.

Both Eqs. (1) and (2) cannot be valid indefinitely since they contain different exponents. It is believed that Eq. (1) is the more applicable expression describing the actual oxidation kinetics, although Eq. (2) appears to be an excellent approximation over the time period studied.

A similar analysis was made on another alloy (50 a/o Cb, 45 a/o Zr, 5 a/o Ti). Experimental and calculated values are shown in Fig. 17.

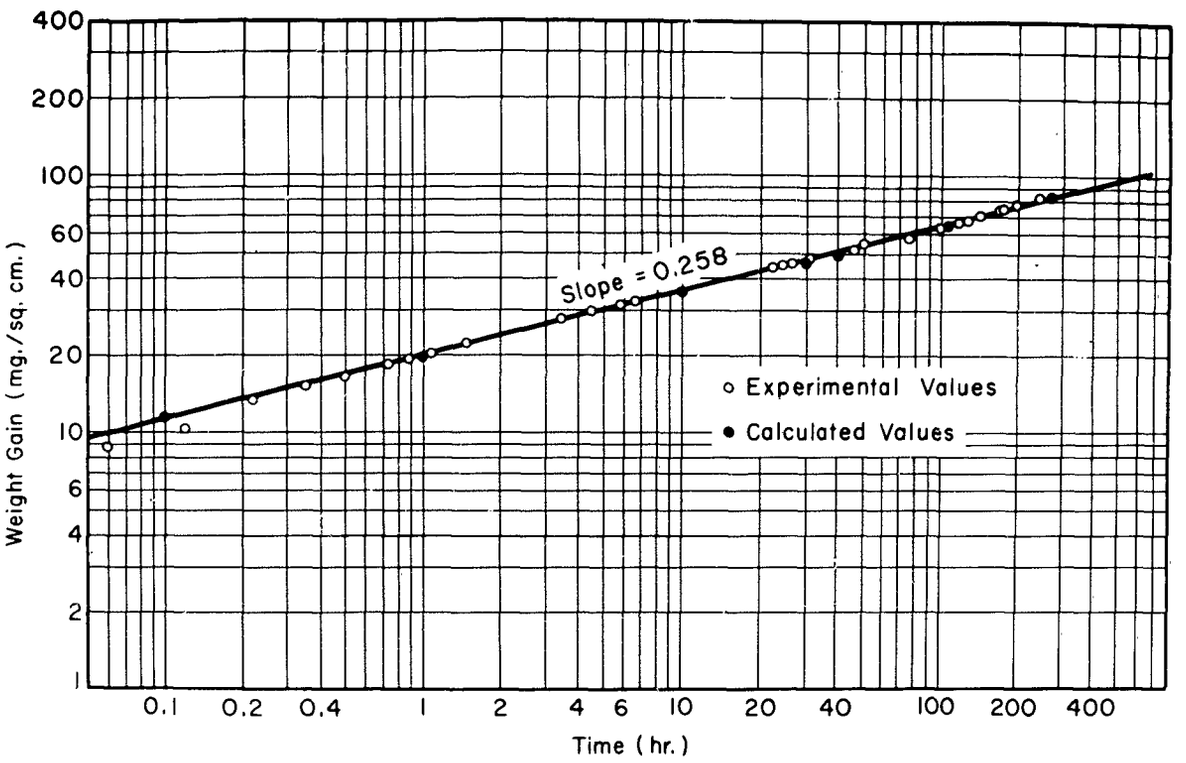

Fig. 16. Weight gain versus time plot for a 50 a/o Zr, 45 a/o Cb, 5 a/o Ti alloy oxidized in air at 1000°C

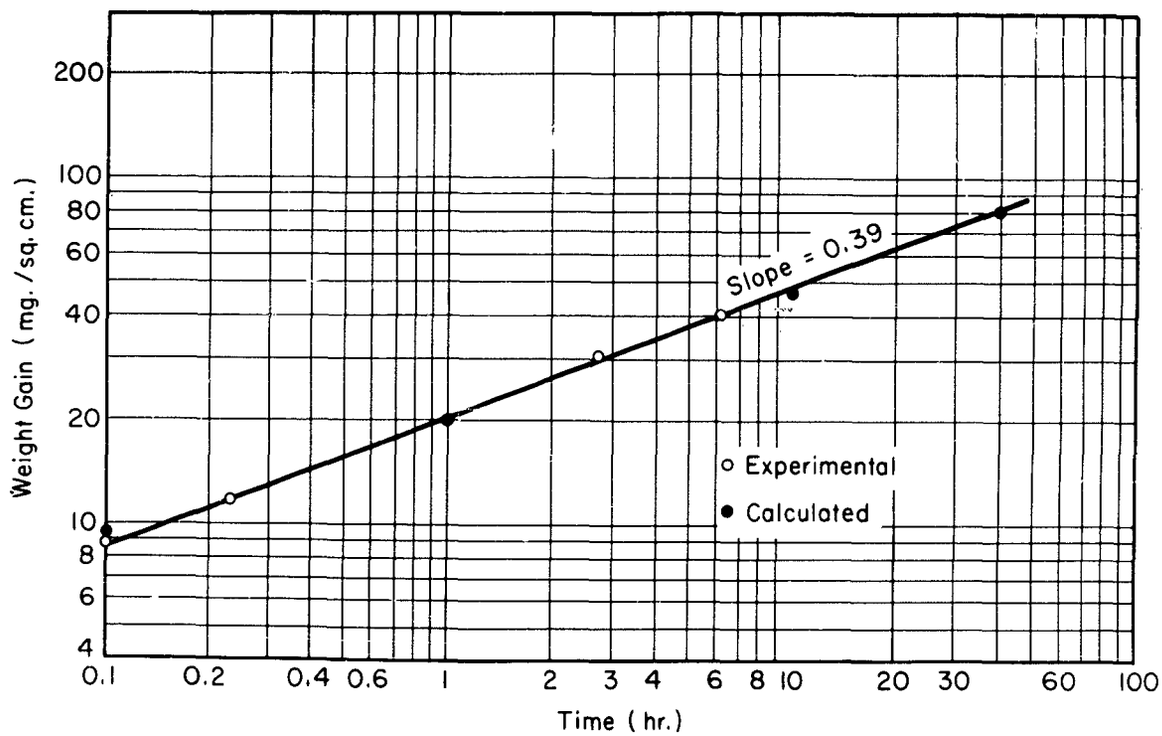

Fig. 17. Weight gain versus time plot for a 50 a/o Cb, 45 a/o Zr, 5 a/o Ti alloy oxidized in air at 1000°C

The values of the external and internal zone exponents were taken from the slopes of the curves in Fig. 18. The kinetic expression for this alloy is as follows:

$$W = \underbrace{3.3t^{0.63}}_{\text{external}} + \underbrace{16.7t^{0.29}}_{\text{internal}}$$

It may be seen that in this case the external oxide scale represents a more significant fraction of the total weight gain and, in fact, in all cases the zone having the greater exponent value will ultimately consume the other zone.

There appears to be a correlation between the zone morphology and the exponent n of both the weight-gain and penetration expressions. The more rapid the variation in coarseness and in volume % ZrO_2 in the oxide dispersion with distance into the alloy, the greater is the deviation in exponent n towards lower values than the normally expected parabolic value of 0.5. This variation may be seen in Figs. 5 and 19.

In Fig. 5 the coarseness varies rapidly with distance and the alloy oxidized according to the relationship, $W = 19.8t^{0.26}$. In Fig. 19, however, the dispersion coarseness remains almost constant and the oxidation expression followed was $W = 31.0t^{0.55}$, an almost parabolic relationship.

The variation in volume fraction was determined by lineal analysis, using the technique described by Howard and Cohen.[5] Knowing the volume fraction of ZrO_2, the oxygen concentration at the internal zone reaction front at a given time, C_o, may be calculated from the

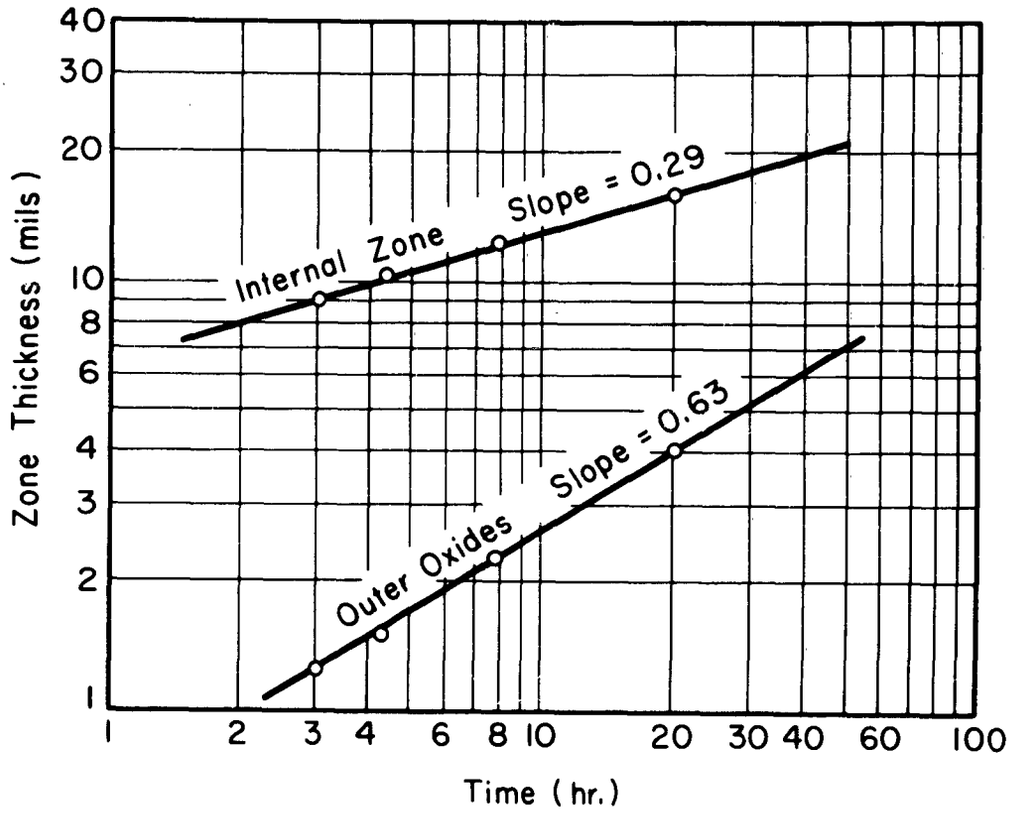

Fig. 18. Zone thickness versus time plot for 50 a/o Cb, 45 a/o Zr, 5 a/o Ti alloys oxidized in air at 1000°C

Fig. 19. Section through a 59 z/o Cb, 40 a/o Zr, 1 a/o Ti alloy oxidized in air for 1.2 hours at 1000°C (2000X)

following expression:

$$C_o = N_{ZrO_2} \cdot \rho_{ZrO_2} \cdot \frac{2 \text{ At. Wt. O}}{\text{Mol. Wt. } ZrO_2}$$

where N_{ZrO_2} is the volume fraction ZrO_2 present at the reaction front at a given time and, ρ_{ZrO_2} is the oxide density. This expression neglects the small quantity of oxygen remaining in the beta solid solution. The variation of oxygen concentration with time for the 50 a/o Zr, 45 a/o Cb, 5 a/o Ti alloy in Fig. 5 is shown in Fig. 20. There is a very rapid initial increase in concentration during the first several hours. The value levels off and gradually approaches the maximum obtainable concentration for the particular ratio of columbium to zirconium in the internal zone.

The time variation in areal fraction of beta solid solution at the reaction front for the above alloy is shown in Fig. 21. The areal fraction decreases rapidly out to several hours and then levels off towards the value of 0.30, the minimum amount obtainable for this alloy if we assume that the ratio of Cb to Zr at the reaction front remains the same as for the over all composition. This minimum value is still not reached at 239 hours at temperature, where the areal fraction is 0.36.

C. TIME AND TEMPERATURE EFFECTS

In the binary alloys investigated, a rapid increase in weight-gain, "breakaway," was observed after several hours at temperature. This is illustrated in Fig. 22 for an alloy oxidized at 1000°C and 1100°C. Visual examination of several specimens which had been

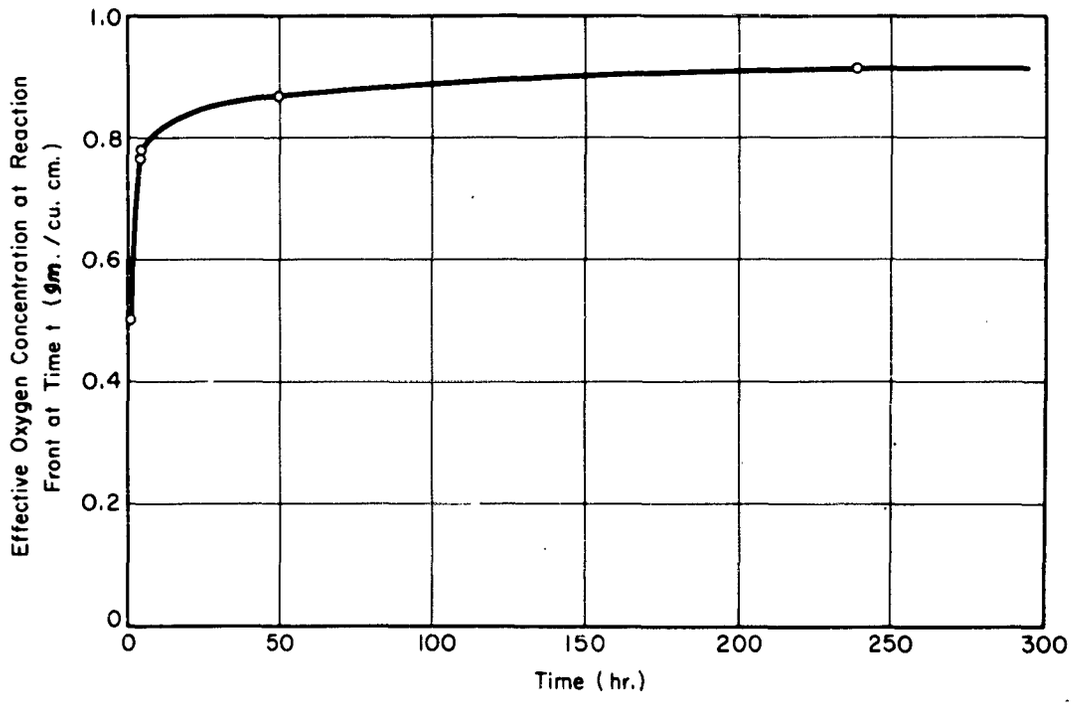

Fig. 20. Effective oxygen concentration at reaction fron versus time plot for a 50 a/o Zr, 45 a/o Zr, 5 a/o Ti alloy oxidized in air at 1000°C

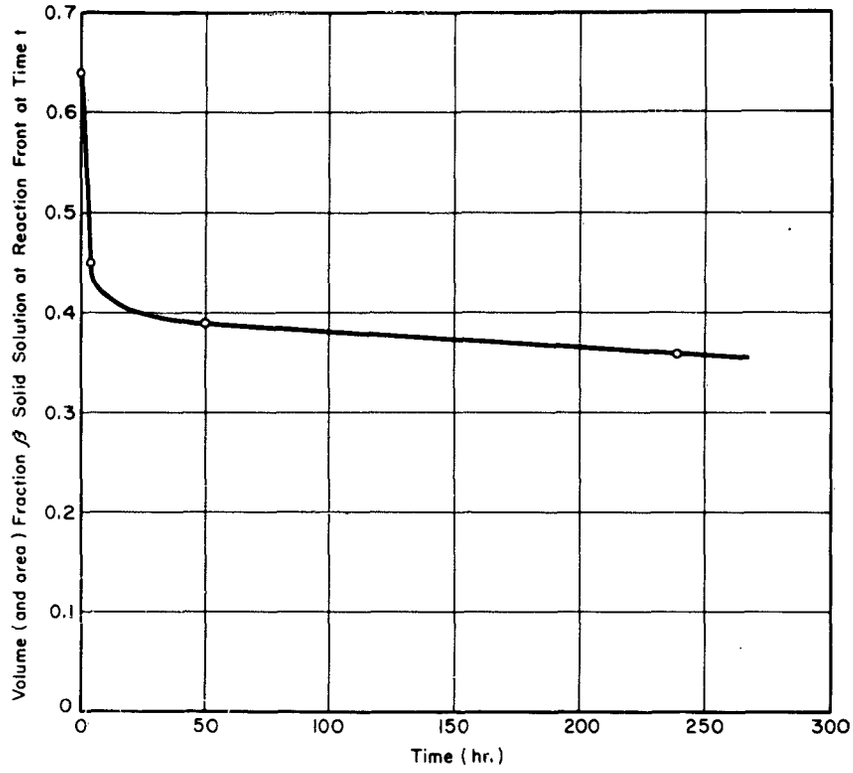

Fig. 21. Volume and area fraction of beta solid solution at reaction front versus time plot for a 50 a/o Zr, 45 a/o Cb, 5 a/o Ti alloy oxidized in air at 1000°C

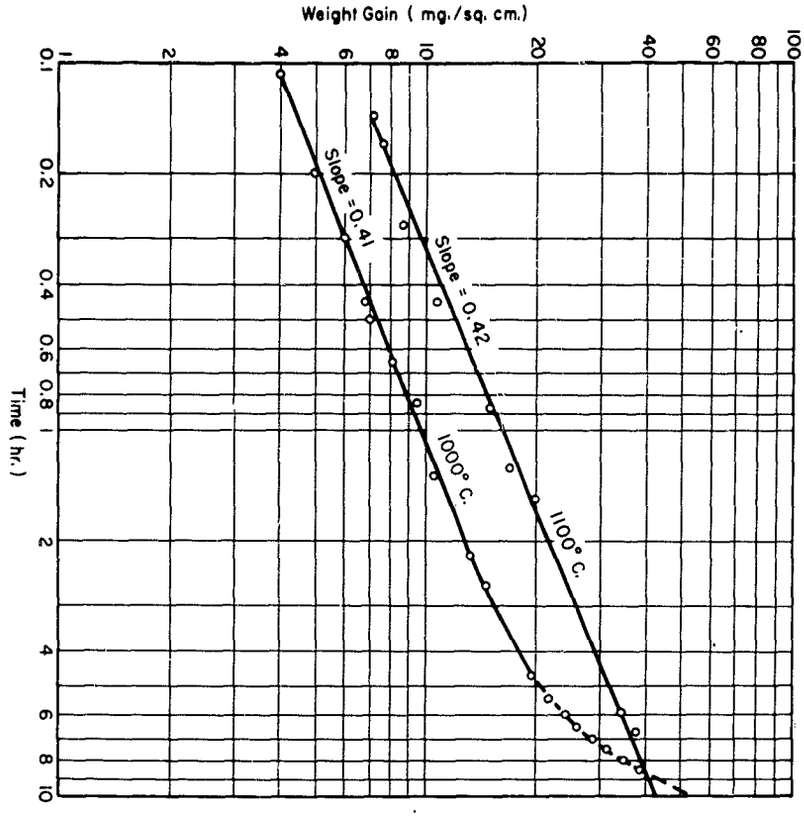

Fig. 22. Weight gain versus time plot for 57 a/o Zr, 43 a/o Cb alloys oxidized in air

oxidized for various times indicated that the increase in slope n was due to a rapid increase in the thickness and porosity of the outer oxide. This phenomenon occurs first at the specimen edges and then spreads to the faces. Figure 23 shows this oxide thickening at the edges of a specimen which had been oxidized for 16.6 hours at 1000°C. It can be seen that the internal zone has been almost entirely consumed in the region of the edge. The data for three binary alloys oxidized at 800°C are shown plotted in Fig. 24. Here again, catastrophic behavior is observed. The times required for the slope to increase are greater at 800°C than at 1000°C. At 1100°C no rapid increase in slope was observed for times up to 17 hours at temperature. This catastrophic phenomenon was not observed in the ternary alloys investigated.

The kinetic behavior of a typical ternary alloy as a function of temperature is illustrated in Fig. 25. There appears to be a minimum in slope at 900°C in the vicinity of the pure zirconium transformation temperature. The value of n rises steeply below this temperature and more gradually above it, although the value at 1100°C, 0.36, is somewhat higher than at 1200°C, 0.32.

An activation energy based on the temperature variation of the rate constant for this alloy was not calculated. The significance of such a calculation is doubtful because of the variable exponent.

A comparison of the relative thicknesses of the various zones after about 23 hours at 1000, 1100, and 1200°C appears in Fig. 26.

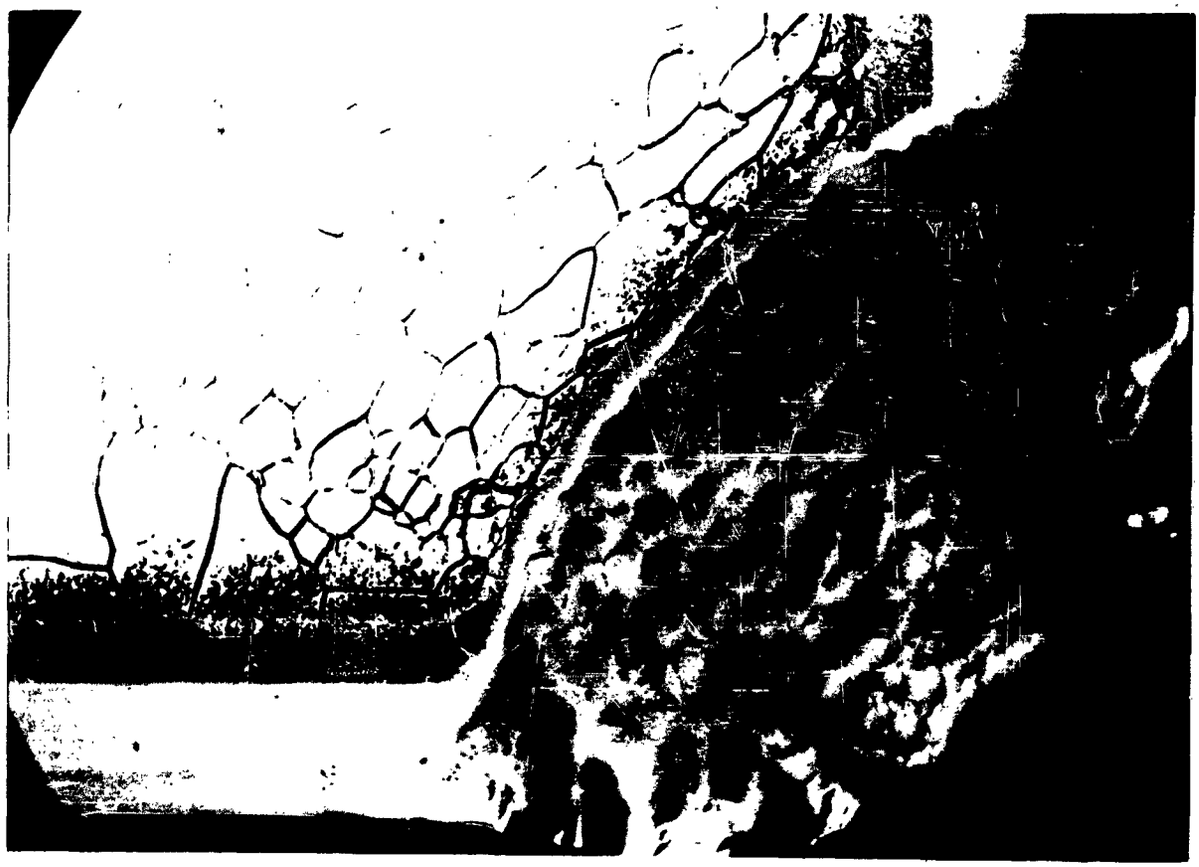

Fig. 23. Section through a corner of a 57 a/o Zr, 43 a/o Cb alloy oxidized 16.6 hours in air at 1000°C (87.5X)

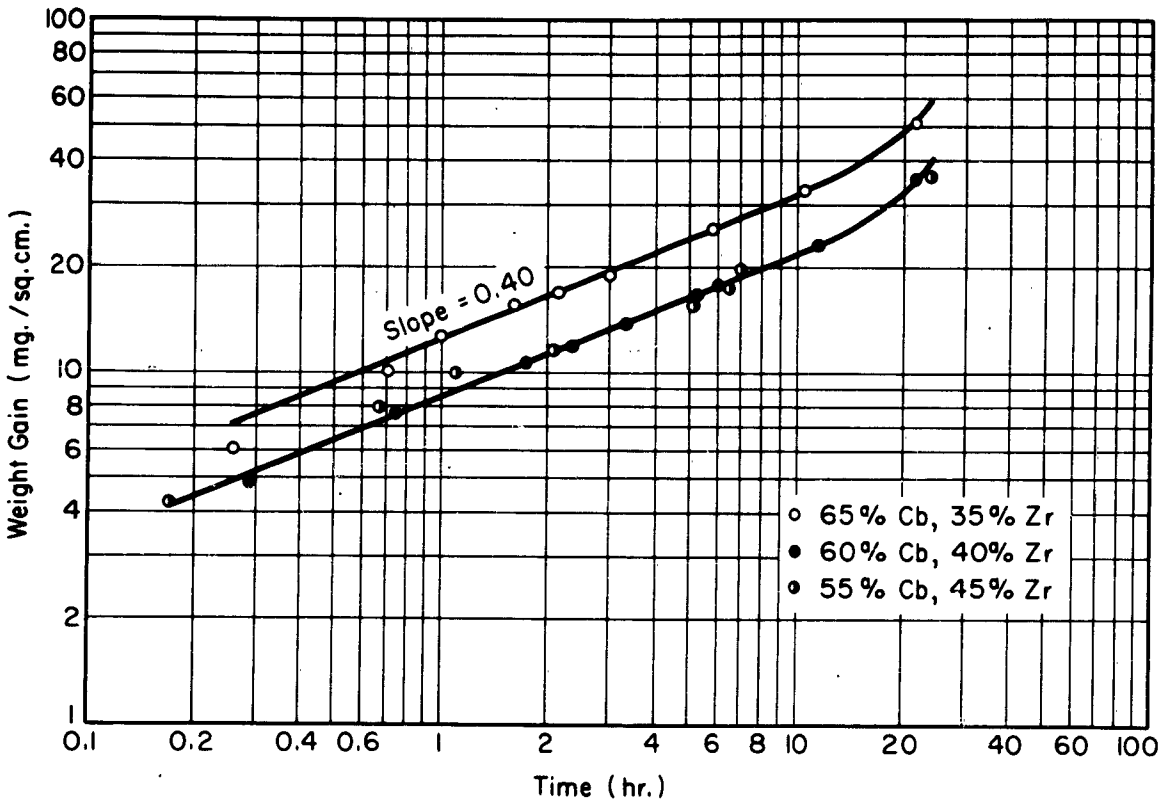

Fig. 24. Weight gain versus time plot for Cb-Zr alloys oxidized in air at 800°C

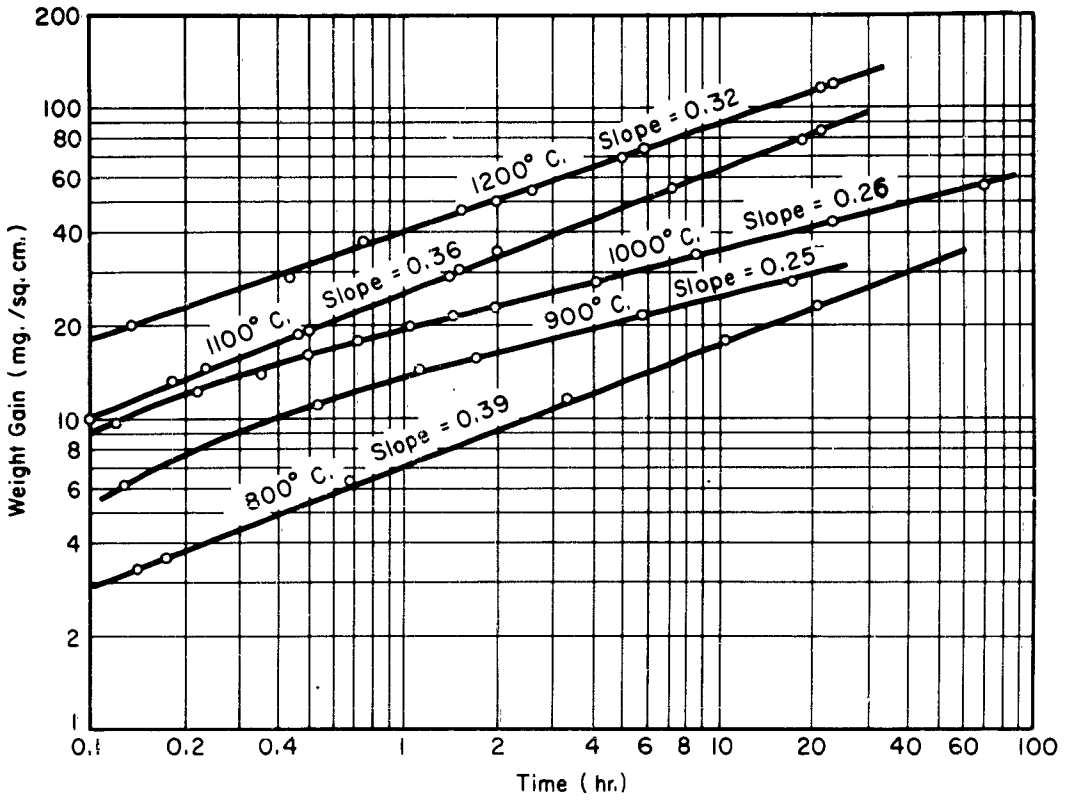

Fig. 25. Weight gain versus time plot for 50 a/o Zr, 45 a/o Cb, 5 a/o Ti alloys oxidized in air at various temperatures

1000° C.

1100° C.

1200° C

Fig. 26. Sections through 50 a/o Zr, 45 a/o Cb, 5 a/o Ti alloys oxidized in air for about 23 hours at various temperatures (100X)

The thickness of the internal zone increases more with increasing temperature than that of the external zones. The specimen oxidized at 1200°C was seriously embrittled and cracked while being mounted in a brass clamp for metallographic polishing. The internal zone existed right to the center of this specimen.

D. PHASE RELATIONS

Since a partially oxidized alloy represents an oxygen-alloy diffusion couple, the order in which the various phases were found to occur on the oxidized alloy could be used to construct a schematic isothermal section at 1000°C of the Cb-Zr-O system. No difference was noted in the kind and order of phases occurring on the binary and ternary (5 a/o Ti) alloys. Therefore, it is believed that an isothermal section through the quaternary Cb-Zr-Ti-O tetrahedron, taken at the 5 a/o Ti level, would appear schematically the same as Fig. 27. This is to be expected since titanium is completely soluble in both columbium and zirconium at 1000°C. However, it is possible that a small amount of titanium oxide was formed but could not be detected by the x-ray techniques used. Further indication that the ternary and quaternary sections are very similar, if not the same was given by metallographic examination, which shows that the binary and ternary alloys have the same general morphology.

Implicit in the construction of the ternary diagram is the assumption that nowhere in the various layers formed does the relative proportion of columbium to zirconium deviate considerably from the preoxidation ratio. This is believed to be a valid assumption during

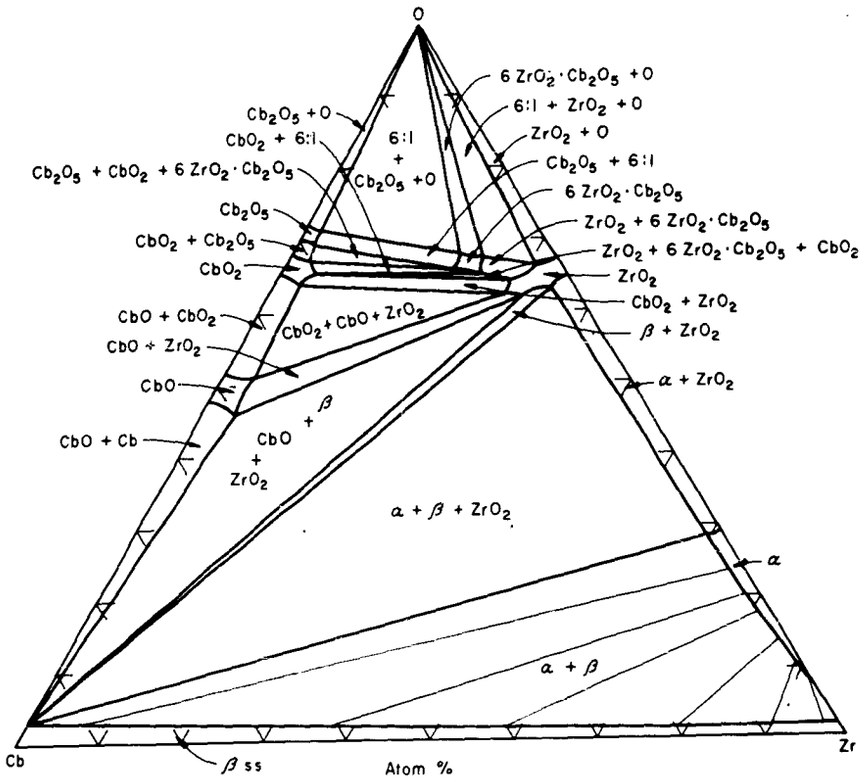

Fig. 27. Schematic Zr-Cb-O ternary phase diagram

the first several hours of oxidation since the diffusivities of columbium and zirconium are probably considerably smaller than that for oxygen. However, variation with time in the ratio of the conjugate phases forming at the internal zone reaction front, Fig. 21, does occur although this does not appear to change the relative order of the phases in the oxidized diffusion couple.

The expected order of the various layers from outside to center produced on Cb-Zr alloys containing 15 to 65 a/o Zr are predicted as follows using the phase diagram, Fig. 27.

$Cb_2O_5 + 6ZrO_2 \cdot Cb_2O_5$

$CbO_2 + 6ZrO_2 \cdot Cb_2O_5$

$CbO_2 + ZrO_2$

$CbO + ZrO_2$

Beta solid solution + ZrO_2

Beta solid solution + alpha solid solution

Beta solid solution

The formation of an internally oxidized region containing ZrO_2 plus beta solid solution is consistent with the available free energy data for the formation of the various probable oxides,[10,11] ZrO_2 being the most stable.

From an x-ray analysis of the residue of a specimen which had been subjected to the chlorination procedure, it was found that the major oxide present on a 50 a/o Zr, 45 a/o Cb, 5 a/o Ti alloy were primarily ZrO_2 and a smaller amount of $6ZrO_2 \cdot Cb_2O_5$. After chlorination all that remained of the specimen was a rectangular shell of the oxide layers. The shell fell apart into a fine powder upon the slightest touch, indicating that it was highly porous.

Under the equilibrium conditions of a diffusion couple, the composition of the beta solid solution in the alpha-plus-beta region should vary from almost pure columbium at the internal zone - core interface to the over all composition at the alpha-plus-beta - beta interface. The latter interface is not generally sharp, however, due to oxygen penetration along grain boundaries. The variation in composition is substantiated by lattice parameter measurements, Fig. 28.

IV. DISCUSSION

A. PROPOSED MECHANISM

This discussion will deal with a proposed mechanism for the oxidation of columbium-zirconium and columbium-zirconium-titanium alloys at temperatures above the allotropic transformation temperature for pure zirconium (862°). The following is a proposed sequence of events occurring when the alloys are oxidized in air.

1. Initially, oxygen is chemisorbed on the alloy surface and goes into solution interstitially. The surface quickly becomes saturated and in some regions the requisite degree of supersaturation is obtained for the following transformation reaction to occur to a limited depth in the alloy.

$$\beta_{(Cb,\ Zr)} \longrightarrow \alpha_{(Zr)} + \beta_{(Cb\text{-rich})} \qquad (I)$$

2. The alpha zirconium formed reacts with oxygen at the surface and in solution, probably as follows:

$$Zr + 2\ O_{(ads)} \longrightarrow ZrO_2 \qquad (II)$$

$$Zr^{+4} + 2\ O^{=} \longrightarrow ZrO_2 \qquad (III)$$

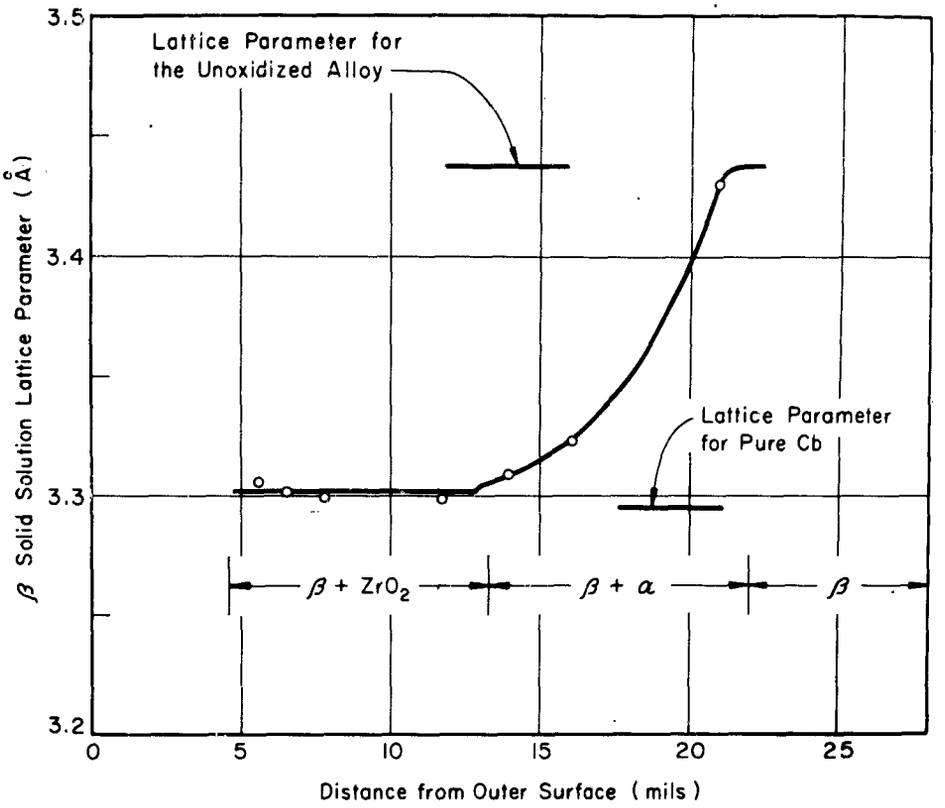

Fig. 28. Beta solid solution lattice parameter versus distance plot for a 50 a/o Zr, 45 a/o Cb, 5 a/o Ti alloy oxidized in air for 26.1 hours at 1000°C

These reactions are known to be highly exothermic.[11] Therefore, the surface temperature may rise above ambient, increasing the diffusion rate and solubility of oxygen in the beta solid solution ahead of the beta, columbium-rich, solid solution plus ZrO_2 region initially formed. Such an increase in the surface temperature above ambient was found by Wasilewski and Kehl[6] during the oxidation of titanium.

3. Simultaneous with the rise in temperature, the columbium in the columbium-rich beta solid solution at the surface probably undergoes the following reactions:

$$Cb + O^{=} \longrightarrow CbO + 2e^{-} \qquad (IV)$$

$$CbO + O^{=} \longrightarrow CbO_2 + 2e^{-} \qquad (V)$$

$$2\ CbO_2 + O^{=} \longrightarrow Cb_2O_5 + 2e^{-} \qquad (VI)$$

Finally, the Cb_2O_5 reacts with the available ZrO_2 to give

$$Cb_2O_5 + 6\ ZrO_2 \longrightarrow 6ZrO_2 \cdot Cb_2O_5 \qquad (VII)$$

Thus, four two-phase layers are formed, three of the layers containing ZrO_2 which was formed by internal oxidation and the fourth, outermost, layer containing either ZrO_2 or Cb_2O_5 plus 6:1, depending on the over all alloy composition.

4. The formation of the surface oxides will decrease the rate of oxygen supply to the region containing alpha zirconium and, if the surface temperature was increased, it will gradually drop toward ambient. The beta phase ahead of the transformed alph-plus-beta region will thus become highly supersaturated and further transformation will occur at an extremely rapid rate, the transformation product having a very fine lamellar structure due to the high degree of supersaturation. If transformation had occurred more slowly, almost all of the zirconium present in the beta

solid solution would have diffused out and formed alpha zirconium, leaving behind pure beta columbium, the equilibrium composition as indicated by the lattice parameter measurements. However, due to the rapidity of the transformation, not all of the zirconium had time to diffuse out of the beta phase to form alpha. The alpha phase forms in very fine platelets, 1200 Å, and reacts rapidly to form ZrO_2. The zirconium remaining in the beta solid solution appears to diffuse to the surface oxide layers, leaving behind almost pure columbium, Fig. 28.

5. During the first minutes of oxidation, the diffusion path through the rate controlling ZrO_2 plus columbium-rich beta solid solution region, the internal oxidation zone, is still relatively short and the rate of oxygen supply is rapid, allowing the supersaturation to build up in the untransformed beta solid solution region ahead of the internal zone. However, with increasing time the rate of oxygen supply decreases, the amount of supersaturation attainable is reduced, and consequently the lamellar transformation product becomes coarser and more plentiful, approaching the equilibrium amount. Therefore, the volume fraction of ZrO_2 at the internal zone reaction front increases with time, while the volume fraction of columbium-rich beta solid solution decreases.

The alpha platelets at the reaction front act as oxygen sinks, taking up oxygen from the beta phase by reacting to form ZrO_2. At 1000°C, for instance, ZrO_2 contains about 26 w/o oxygen, whereas saturated alpha contains only 6.5 w/o[12], and saturated beta contains a maximum of about 0.7 w/o.[13] The oxygen consumed in the reaction at the front would otherwise penetrate into the alloy and extend the alpha plus beta region. Since the volume fraction of alpha phase

at the front, and consequently the concentration of oxygen, is continuously increasing with time, the velocity of the front decreases at a faster rate than it would for normal parabolic penetration.

In addition, the oxygen uptake is proportional to the cross-sectional area through which diffusion can occur. If we assume that oxygen diffusion in the internal zone is occurring predominately in the beta phase, then the oxygen uptake will be less than would occur at constant area since the area of the beta phase parallel to the outer surface is continually decreasing with time.

B. EFFECT OF ZIRCONIUM

The effect of increasing the zirconium content of binary alloys on the oxidation equation exponent, n, may be seen in Fig. 13. The exponent drops off continuously between 0 and 10 a/o zirconium from about 0.79 to 0.53 and remains at 0.53 up to 45 a/o zirconium.

Between 45 and 50 a/o zirconium, there is a more rapid drop-off, the value of n levelling at about 0.4. In the case of these binary and ternary alloys, two competing processes are occurring, one process tending to lower the value of n and the other to raise it.

The lowering process is the one described above which is dependent on the time variation in the volume fraction of ZrO_2 at the internal zone reaction front. The degree of variation appears to increase with zirconium content, reaching a maximum between 45 and 50 a/o zirconium.

On the other hand, the exponent is increased by the formation of a voluminous semiprotective outer scale toward a value between 0.5 and 1.0, depending on the degree of protectivity of the scale.

Increasing the zirconium content beyond about 10 a/o increases the degree of protectivity of the outer scale, but at the same time the weight gain after one hour is increased considerably at zirconium contents of less that 35 a/o. Thus, at very low zirconium contents, 1 to 10 a/o zirconium, the oxide formed, Cb_2O_5 is completely nonprotective and, in fact, at 1000°C the alloys oxidized at a considerably faster rate than does pure columbium. This is partly due to the large ionic radius, 0.79 A°, of Zr^{+4} as compared to 0.69 A° for Cb^{+5}.[9] The increased size effect when zirconium substitutes for columbium in the Cb_2O_5 lattice accentuates the already large volume ratio, 2.69, and increases the tendency of the oxide to blister and crack. In addition, the plus four valence of the zirconium ion tends to increase the diffusion rate through the oxygen deficit Cb_2O_5 scale.

With increasing zirconium content, the oxidation rate constant drops off rapidly and reaches a minimum at about 55 a/o zirconium. The drop-off in rate constant comes about as the ratio of $6ZrO_2 \cdot Cb_2O_5$ to Cb_2O_5 in the outer scale increases, the double oxide being of a more protective nature than the Cb_2O_5. Figures 8 and 9 show the effect of zirconium on the outer oxide scale. The formation of the outer oxides occurs by the consumption of the internally oxidized zone, probably according to reactions (IV) through (VII)

indicated previously. The rate at which the internal zone is consumed increases markedly in the alloys containing more than 30 a/o Zr after the outer oxide reaches a critical thickness (breakaway). This thickness is first reached at the specimen edges.

C. EFFECT OF TITANIUM

The addition of titanium to columbium-zirconium alloys appears to have a dual effect on the oxidation behavior. First, titanium mechanically stabilizes the outer oxide scale, allowing it to grow to a greater thickness while remaining protective. Second, it reduces appreciably the rate of consumption of the $\beta_{(Cb\text{-}rich)}$ solid solution in the internal zone. The consumption occurs by the formation of CbO and its subsequent reaction to form higher oxides. Titanium has a similar beneficial effect on the oxidation behavior of pure columbium,[4] where the addition of 10 a/o titanium reduces the diffusivity of oxygen in the metal by one order of magnitude at 1000°C and decreases the oxidation weight gain rate constant to 1/3 of the pure columbium value.

By stabilizing the outer oxide scale and slowing down the consumption rate of the internal zone, increasing titanium content, up to about 10 a/o, decreases the value of the exponent n for a given zirconium content as may be seen in Fig. 14. It also suppresses the breakaway phenomenon, at least out to longer times than employed in this investigation. By decreasing the rate of consumption of the internal zone, titanium additions allow the internal

zone to grow considerably thicker, increasing the oxygen diffusion path and causing a greater variation in ZrO_2 dispersion coarseness, the factor which appears to be most responsible for the decreased exponent.

D. SIGNIFICANCE OF THE EXPONENT, n

If the above analysis is correct, then no special significance may be attached to any particular value of n for the internally oxidized alloys studied. Instead, n is a variable related to (1) the rate and mode of growth of the external oxide scale and to (2) the rate and mode of growth of the internal zone which appears to be a function of the time rate of variation in morphology and quantity of the dispersed phase.

Both of the above factors are controlled by the alloy composition and oxidation temperature and thus, so is the exponent n.

Even aside from the above considerations, the above considerations, the value of n for a given composition oxidized at a given temperature would be expected to vary after long times at temperature. This variation comes about since the total oxidation weight gain of a given sample can be divided into a series of terms, each term representing the growth kinetics of a particular layer. If we consider the "external" oxide scale and the internally oxidized zone, as the two layers in which the weight gain occurs, then

$$W = k_1 t^{m1} + k_2 t^{m2} \qquad (1)$$

where W represents the total weight gained up to time, t, and k_1, m_1 and k_2, m_2 are constants for the outer scale and the internal zone, respectively. It was shown previously that this type of expression gives excellent agreement with the experimentally determined data over the time range studied. If a log-log plot of the above expression is made, it will become evident that a straight line of slope n will be approximated for long times only when one term is small in comparison with the other. Since the relative magnitudes of the two terms will in general change with time, it may be seen that this expression can be approximated by a straight line on such a plot only over a limited time range, although this range may be appreciable. Thus, the equation

$$W = kt^n \qquad (2)$$

is only an approximation for the alloys studied, unless n is considered to be a variable.

Equation (1) allows us to gain some insight into the possible mechanisms by which zirconium additions up to 10 a/o can cause a very considerable increase in the oxidation rate constant of pure columbium while at the same time decrease the oxidation exponent n to the so-called "parabolic" value, Figs 13 and 14. The fact that pure columbium oxidizes so that m_1 of Eq. (1) equals 0.79 at 1000°C indicates that Cb_2O_5 is semiprotective in nature, possibly due to the oxides being adherent and not "completely" porous at temperature. Of course, for pure columbium, k_2 must be extremely small since internal

oxidation cannot occur in a pure metal and since the oxygen solubility in columbium is very limited, being about 0.7 w/o at 1000°C.[7]

The addition of up to 10 a/o zirconium appears to increase the values of k_1, m_1, and k_2, while decreasing the value of m_2, the net effect being to increase the total one-hour weight gain while reducing the over all exponent, n. The increase in k_1 might come about due to an elevation in surface temperature above ambient, caused by the exothermic ZrO_2 formation reaction or due to the formation of a completely nonprotective outer oxide. Beyond 10 a/o zirconium it is not obvious how the two terms on the right hand side Eq. (2) vary with composition so as to keep the over all exponent equal to about 0.53. However, since the outer oxide is becoming more protective at higher zirconium contents, it is possible that the oxygen supply to the internal zone is decreased, thus decreasing k_2 as well as k_1 out to about 45 a/o zirconium. Beyond this composition, k_2 becomes the more significant term and the over all exponent drops further to a value of 0.40.

E. EFFECT OF AREA AND DENSITY

A point which, in general, should be considered is the change in reaction surface area of a rectangular prism specimen brought about by the oxygen penetration normal to a given face. On very small specimens, this effect becomes appreciable when the oxide thickness becomes large. However, the specimens used in this investigation were sufficiently large to allow this effect to be neglected, except possibly at very long times.

The changing density of the internal zone should also be considered. The formation of ZrO_2 will tend to decrease the over all density since ZrO_2 occupies about 50% more volume than the equivalent quantity of pure zirconium. This decreased density manifests itself as only a slight increase in sample dimensions, because the effected zone represents only a small percentage of the total sample volume. If sufficiently small specimens were used, or if the internal zone became relatively thick, this effect would become appreciable.

F. QUANTITATIVE KINETIC EXPRESSION

It appears extremely difficult to express the highly varied oxidation behavior of the internally oxidized zones observed in this study by means of any one fundamental quantitative expression. However, the empirical expression developed by Meijering and Verheijke[8] to describe the kinetics of the conversion in air of Cu_2O to CuO might also be applied here. This process was found to follow a "cubic" rate expression. If we assume that the oxygen flux is inversely proportional to X, the effective diffusion path, then

$$\frac{dM}{dt} = \frac{-ADk'}{X} \qquad (5)$$

where M is the internal zone weight gain per unit of original surface area, A is the effective area through which oxygen diffusion is occurring at time, t, D is the diffusivity of oxygen in the internal zone, and k' is a constant. Further, if we assume an exponential time variation in the product AD similar to that developed by Meijering and

Verheijke for the variation of D alone, and that M is proportional to X, then Eq. (5) can be put into the following form:

$$\frac{dX}{dt} = \frac{K\{f + (1-f)\exp(-kt)\}}{X} \qquad (6)$$

Upon integration, Eq. (6) becomes:

$$X^2 = 2(1-f)\frac{K}{k}\left\{1 - \exp(-kt) + \frac{f}{1-f} kt\right\} \qquad (7)$$

For values of the parameter $\frac{f}{1-f}$ between 0.3 and 0.5, a plot of X^3 versus t yields nearly a straight line at high and low values of kt. By varying the parameter between 0.5 and 0.05, n can be made to vary from 0.33 to 0.21 for intermediate values of kt.

However, M was assumed proportional to X in formulating Eq. (6), whereas the oxygen concentration in the internal zone does vary with X, especially in the early stages of oxidation, Fig. 20. Therefore, Eq. (6) is, at best, an empirical approximation to the actual oxidation kinetic behavior.

It may be concluded that the highly varied and complex oxidation behavior undergone by the alloys studied makes it extremely difficult to predict beforehand the particular values of the rate constant k and the oxidation exponent n for any given composition oxidized at a particular temperature. Thus, it is still necessary to determine the oxidation kinetics for a given alloy experimentally. Once the kinetic data have been determined, they may be approximated by an empirical relationship, Eq. (1), involving two weight-gain terms, one term for the external scale and the other for the internally oxidized region. When these two terms possess nonparabolic exponents (less than 0.5) they may also be described mathematically by Eq. (7) over a limited time range.

V. ACKNOWLEDGMENT

The authors wish to acknowledge Dr. George St. Pierre for his valuable advise and helpful discussions. The financial support received from Universal-Cyclops Steel Corp., International Nickel Company and The Office of Naval Research was greatly appreciated.

REFERENCES

1. H. M. McCullough, F. H. Beck, and M. G. Fontana, "Formation of Oxides on Some Stainless Steels at High Temperatures," Trans. ASM, 43, 404 (1951).

2. E. W. Colbeck, S. W. Craven, and W. Murray, "The Chlorine Method of Separating Non-Metallic Inclusions in Steel," Iron and Steel Institute Special Report No. 16, 124 (1937).

3. M. Hansen, Constitution of Binary Alloys, McGraw-Hill Book Co., Inc., New York (1958)

4. C. T. Sims, W. D. Klopp, and R. I. Jaffee, "Studies of the Oxidation and Contamination Resistance of Binary Niobium Alloys," ASM Preprint No. 70 (1957).

5. R. T. Howard and M. Cohen, "Quantitative Metallography by Point-counting and Lineal Analysis," Trans. AIME, 172, 413 (1947).

6. R. J. Wasilewski and G. L. Kehl, "Diffusion of Nitrogen and Oxygen in Titanium," J. Inst. Metals, 83, 94 (1954-55).

7. A. U. Seybolt, "Solid Solubility of Oxygen in Columbium," J. Metals, 6, 774 (1954).

8. J. L. Meijering and M. L. Verheijke, "Oxidation Kinetics in the Case of Ageing Oxide Films," Acta Met., 7, 331 (1959).

9. F. Laves, Theory of Alloy Phases, ASM, Cleveland (1956).

10. A. Glassner, "A Survey of the Free Energies of Formation of the Fluorides, Chlorides, and Oxides of the Elements to 2500°K," ANL-5107, August 1953.

11. J. P. Coughlin, "Contributions to the Data on Theoretical Metallurgy, XII. Heats and Free Energies of Formation of Inorganic Oxides," U.S. Bureau of Mines, Bulletin 542 (1954).

12. R. F. Domagal and D. J. McPherson, "System Zirconium-Oxygen," Trans AIME 203, 1034 (1954).

13. A. V. Seybolt, "Solid Solubility of Oxygen in Columbium," J. Metals, 6, 774 (1954)

PUBLICATIONS

1. Tech. Report 467-5, "Oxidation Characteristics of Columbium Alloys," G. Gordon, C. Scheuerman, and R. Speiser. ONR Contract N60nr22528-NR039-005. March 1959. Ohio State University Research Foundation .

2. U.S. Patent, 2,985,531; "Niobium-Zirconium Base Alloy." G. M. Gordon, Rudolph Speiser, and J. W. Spretnak Assignors to the Ohio State University Research Foundation

3. "Oxidation Resistance of a Cb-Zr-Ti Alloy," G. M. Gordon, J. W. Spretnak and Rudolph Speiser, Trans. AIME, October, 1958, p. 659.

Investigator _____ Date _____

Supervisor Rudolph Speiser Date Oct 31, 1961

For The Ohio State University Research Foundation

Executive Director Orame C. Woolpert Date 31 Oct 1961

AS